Submitted, ACS Synthetic Biology, Sep 2013
http://www.cds.caltech.edu/~murray/papers/sun+13-acs_synbio.html

Linear DNA for rapid prototyping of synthetic biological circuits in an *Escherichia coli* based TX-TL cell-free system

AUTHORS:

Zachary Z. Sun[1], Enoch Yeung[2], Clarmyra A. Hayes[1], Vincent Noireaux[3], Richard M. Murray[1, 2]

[1] Division of Biology and Biological Engineering, California Institute of Technology, Pasadena, CA, USA
[2] Department of Control and Dynamical Systems, California Institute of Technology
[3] School of Physics and Astronomy, University of Minnesota, Minneapolis, MN, USA

CORRESPONDING AUTHOR: Zachary Z. Sun, zsun@caltech.edu.

ABSTRACT:

Accelerating the pace of synthetic biology experiments requires new approaches for rapid prototyping of circuits from individual DNA regulatory elements. However, current testing standards require days to weeks due to cloning and *in vivo* transformation. In this work, we first characterized methods to protect linear DNA strands from exonuclease degradation in an *Escherichia coli* based transcription-translation cell-free system (TX-TL), as well as mechanisms of degradation. This enables the use of linear DNA PCR products in TX-TL. We then explored methods to calibrate linear DNA to plasmid DNA by concentration. We also demonstrated assembly technology to rapidly build circuits entirely *in vitro* from separate parts. Using this strategy, we prototyped a four-piece genetic switch in under 8 hours entirely *in vitro*. Rapid *in vitro* assembly has applications for prototyping circuits of unlimited size when combined with predictive computational models.

KEYWORDS:

Rapid prototyping, TX-TL, cell-free expression, synthetic biology, biomolecular breadboard, synthetic gene circuits

INTRODUCTION:

The current mode of building synthetic circuits relies heavily on *in silico* design followed by *in vivo* testing and revision. Complete circuits are cloned into a plasmid for propagation *in vivo*, a labor-intensive and serial process that has a 1-week testing cycle, which scales poorly for complex circuits (Fig. 1a) [1-3]. Although large-scale successes have been accomplished by this testing method, there is a significant time cost to this engineering cycle. For example, the industrial production of artemisinin from synthetic circuits in *E. coli and S. cerevisiae* has taken 150 person-years, of which much time can be attributed to part testing [4, 5].

This current process ignores a commonly applied principle in engineering: testing of circuits in a simplified prototyping environment, such as a breadboard, to decrease complexity and increase

iteration speed. One experimental platform for a simplified *in vivo* environment is cell-free protein synthesis systems, which are known for ease-of-use and well-defined features [6-8]. Circuits such as oscillators, switches, and translational regulators [9-11] have been implemented either in reconstituted cell-free systems, which lack significant similarity to the *in vivo* environment, or in S30 extracts optimized for protein production in lieu of circuit design [12, 13]. The ideal cell-free expression system should act as a "biomolecular breadboard" intermediary between circuit testing and *in vivo* implementation. It should mirror the *E. coli in vivo* state while preserving protein production capability and regulatory mechanisms [14].

We propose an S30-based transcription-translation system (TX-TL) that we have developed to serve as part of a biomolecular breadboard. This system is currently supported with characterizations of transcriptional and translational processes, a usage toolbox, models, and protocols for creation and use [14-18]. We have also demonstrated simple logic gates, cascades, and large-scale assembly of bacteriophage [14, 19]. While most circuits implemented in TX-TL are run off of plasmids to avoid exonuclease degradation from endogenous RecBCD, linear DNA can be protected from degradation with the RecBCD inhibitor bacteriophage lambda gam protein both *in vivo* and in other S30 extracts [20, 21]. The ability to run circuits off of linear DNA opens up possibilities for rapid prototyping, as linear DNA can be created in high yields either synthetically or entirely *in vitro* in just a few hours. Linear DNA also enables applications not possible with plasmid DNA, such as the expression and analysis of toxic proteins.

In this paper, we establish linear DNA as a mode for rapid prototyping in the biological breadboard (Figure 1b). We first develop protective mechanisms to make linear DNA expression comparable to that of plasmid DNA. We also verify recent findings in other S30 extracts suggesting transcriptional processes using linear DNA are disparate from those using plasmid DNA [22]. To compensate for these differences, we calibrate linear DNA results to plasmid DNA results through experimental data and demonstrate circuit dynamics are similar for a genetic switch on linear and plasmid DNA. A rapid, entirely *in vitro* assembly technique is then developed to assemble regulatory elements and basic circuits from standard or custom pieces in under 4 hours, with complete testing in under 8 hours. By maintaining an engineering cycle time of 8 hours or less, our technology allows for prototyping of circuits of unlimited size in a standard business day.

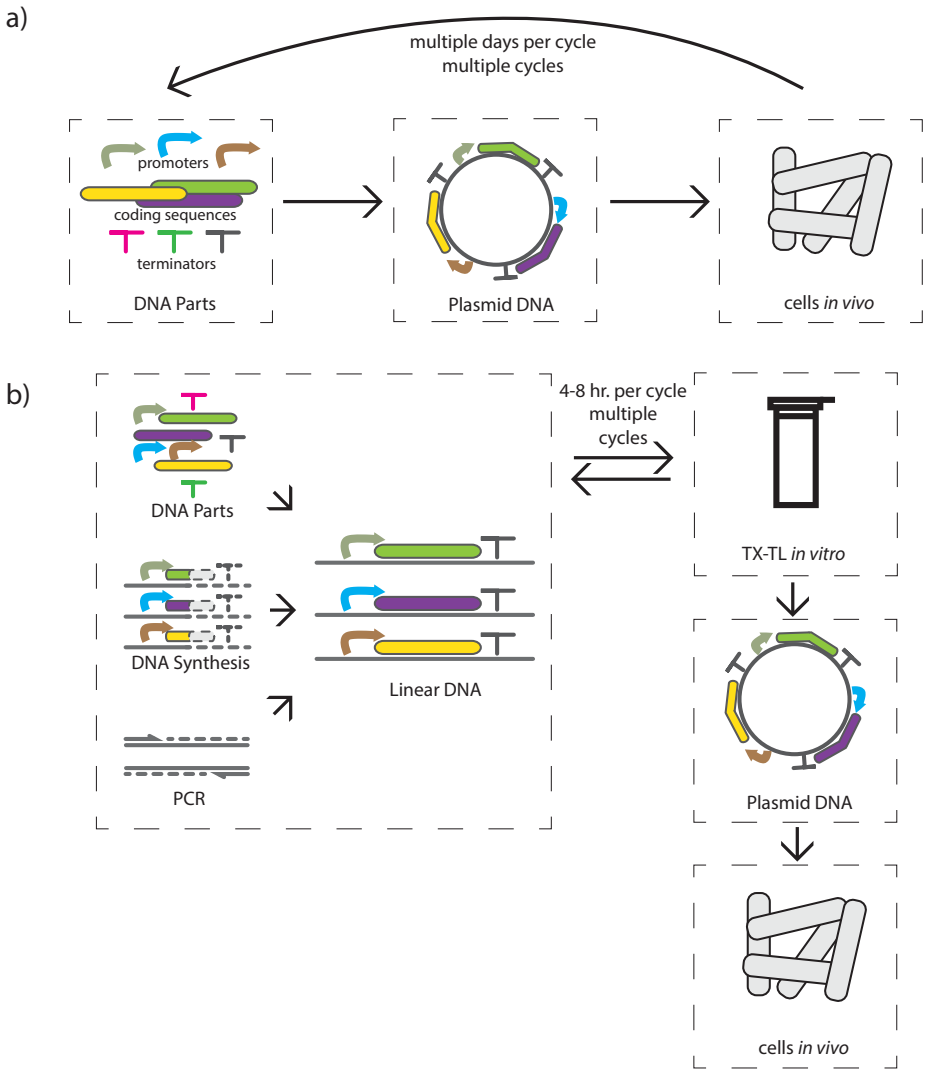

Figure 1. Overview of rapid prototyping procedure of gene circuits. a) Traditional testing of circuits, where parts are cloned onto a single plasmid or sets of complementary plasmids, tested *in vivo*, and cycled back to construction. b) Rapid prototyping procedure, where circuits are cycled between construction on linear DNA and testing in TX-TL. When a final circuit prototype is completed, only 1 cycle occurs of plasmid DNA construction and circuit implementation *in vivo*.

RESULTS AND DISCUSSION:

Linear DNA can be protected for expression in TX-TL

We initially sought to characterize the stability of linear DNA in TX-TL. Integral to this is accurate quantification of both linear and plasmid dsDNA concentration, as large errors in quantifying small amounts of dsDNA is known to introduce significant downstream bias [23]. This is especially true for TX-TL, as experiments can require less than 10 ng/μL of stock dsDNA. Two methods for dsDNA quantification commonly in use include spectrophotometry and fluorometry. We compared both and established guidelines for measuring linear and plasmid DNA concentrations (Supplemental S1, Figure S1, Table S1).

Unless otherwise stated, all experiments in the paper were done with a single extract batch to avoid extract-to-extract variation [14]. Additionally, all DNA sequences used can be found in Supplemental Information and on NCBI GenBank or the Addgene depository (Supplemental S2).

In order to determine ideal conditions for expression of a linear DNA template, we compared the production of fluorescent reporter deGFP from plasmid pBEST-OR2-OR1-Pr-UTR1-deGFP-T500 to that of the 810 bp linear DNA product with no steric protection on the 5' or 3' end. This plasmid was previously optimized for high expression in TX-TL [16]. 16 nM of linear DNA produced 1.25% the deGFP endpoint concentration of plasmid DNA (Figure 2a). In order to use lower concentrations for prototyping, we explored the addition of purified lambda gam to protect DNA from exonuclease degradation. Although protocols to purify lambda gam exist, the storage buffers are toxic to TX-TL reactions [20]. We first conducted a toxicity assay of common protein storage buffer additives in an alternate extract and determined a compatible non-toxic storage buffer (Figure S2, Figure S3). Notably, glycerol as a cryoprotectant is highly toxic to TX-TL and required replacement with DMSO. With lambda gam protein present in the reaction, deGFP concentration from 16nM of linear DNA recovered to 37.6% of plasmid DNA (Figure 2a).

To determine a working concentration for lambda gam protein, we compared the protective ability of dilutions of purified protein on 2 nM of linear DNA without steric protection, and found an optimal working concentration of 3.5 μM (Figure 2b). We used this concentration for subsequent experiments. 3.5 μM is likely significantly above saturating amount, as at 3.5 μM and above the incubation of lambda gam with crude extract did not improve expression, while below 3.5 μM incubation time improved expression (Figure S4). While purified lambda gam improved linear DNA expression, it showed no toxicity to plasmid DNA expression (Figure 2c).

We also conducted a saturation curve of plasmid and linear DNA by measuring endpoint deGFP concentration as a function of DNA concentration. Using this data, we defined a linear regime and saturation regime (Figure S5). In the linear regime, a doubling of DNA concentration produces a doubling of signal, implying no resource limitation due to polymerase and ribosome saturation or resource depletion (rNTPs, amino acids). Resource limitation occurs in the saturation regime, where increased DNA marginally increases signal. For most circuits, running in the linear regime of DNA concentration is important to avoid resource limitation affects. While plasmid DNA enters the saturation regime above 4 nM, linear DNA remains in the linear regime up to 16 nM (Figure 2c). This established a typical working concentration for linear

DNA, and suggested the ability to calibrate linear DNA results to plasmid DNA results by concentration.

With the presence of lambda gam protein, we also tested steric protective mechanisms to inhibit degradation by RecBCD and other exonucleases [21, 24]. We first tested two independent non-coding sequences flanking the ends of our linear cassette (Figure 2d). "Sequence 1" was derived from the original plasmid, while "Sequence 2" is from the coding sequences of two long *E. coli* genes, *gltB* and *lhr*, presumed to have no large internal reading frames. Protection from the sequences tended to be both sequence-specific and length-dependent. 5 bp of protective sequences on each end increased signal 2.4-fold over no protective ends, suggesting the importance of short sequences for either sigma-70 binding or for buffering the promoter from exonuclease degradation. Protection reached a maximum around 250 bp-500 bp, with 6-fold larger signal over no steric protection. Therefore, unless otherwise specified we used 250 bp of protective sequences for subsequent linear constructs. We also tried protecting linear DNA with 1, 2, or 5 phosphorothioate modifications at the 5' end added by PCR, and found improvement only when 5 bp or less of non-coding DNA protection was present (Figure S6a). Interestingly, 5 phosphorothioates on the 0 bp protection construct significantly changed the dynamics of expression, supporting the hypothesis that shorter ends interfere with sigma-70 binding and suggesting a minimum protective length of 15 bp from the -35 promoter region (Figure S6b).

DNA degradation in TX-TL is incomplete from the 5' or 3' end

While it is known that RecBCD degradation occurs from the 3' end, little is known about degradation of ensemble populations of DNA [25]. This is functionally important for design of linear DNA constructs. After determining methods of protecting DNA through indirect assays, we wanted to directly measure DNA concentration over the linear regime of a TX-TL reaction. To do so, we labeled a typical non-saturating amount of linear DNA (2 nM, 25 ng) with a fluorescent probe, AlexaFluor-594, in a complementary spectrum to the deGFP reporter. We first incorporated the probe randomly throughout the linear DNA by PCR using an AlexaFluor-594-5-dUTP, which implemented in the DNA in the place of dTTP (Figure 3a). Despite the labeling, linear DNA retained expression ability as measured by deGFP signal. Negligible DNA was degraded within 1 hour and over 75% remained within four hours when templates were protected by lambda gam, suggesting minimal degradation of template over the useful period of data collection. We also labeled the same template only at the 5' end through PCR by using primers with AlexaFluor-594 covalently bound (Figure 3b). While expression of deGFP was equally conserved, significant degradation of AlexaFluor-594 signal was seen when compared to labeling throughout the linear DNA. We concluded that in the ensemble reaction in the presence of lambda gam, RecBCD exonuclease in the reaction caused incomplete degradation at the 5' or 3' end. RecBCD is unable to complete degradation of a complete linear template. This is supported by previous data showing that steric protection was most effective with small amounts of DNA (Figure 2d), as well as evidence suggesting the existence of always-active RecBCD complex despite saturating lambda gam concentration [26]. To our knowledge, this is the first evidence of a RecBCD degradation mechanism with ensemble linear DNA.

We also determined that degradation of linear DNA is a saturated process limited by the amount of active RecBCD complex. We conducted the same degradation assay, but using saturating

amounts of DNA (250 ng, 20 nM) and saw no significant degradation at 120 minutes in the presence of lambda gam (Figure S7). Degradation also seemed invariant to extract preparation conditions. We also made an extract prepared at 29°C, based on previous work where lower preparation temperature decreased exonuclease activity on linear DNA [27]. However, we saw no decreased degradation. Based on these findings, we concluded that linear DNA remained present throughout the TX-TL reaction, and at high concentrations or with sufficient steric protection could be completely protected against exonuclease degradation.

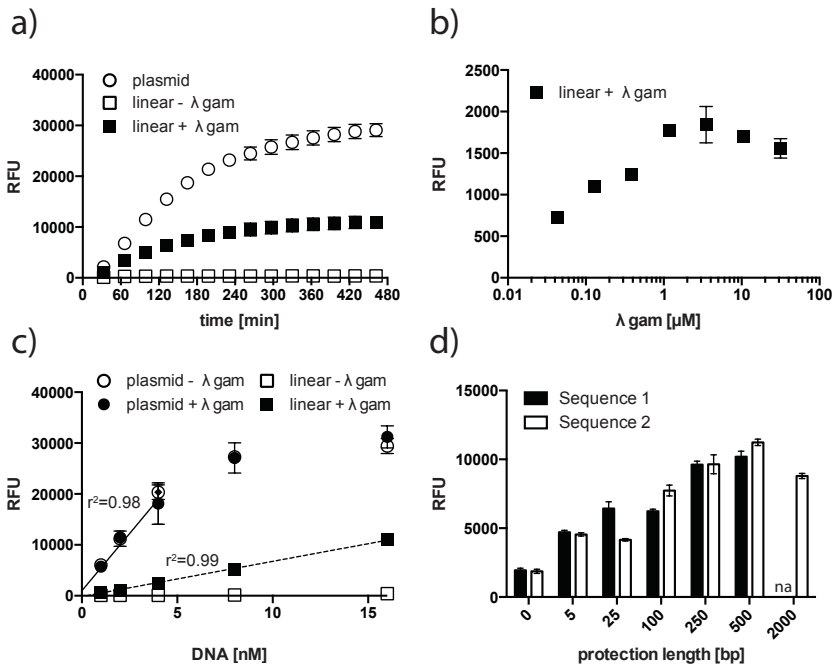

Figure 2. Protection of linear DNA from degradation in TX-TL. a) Comparison of deGFP time-series fluorescence for plasmid DNA, linear DNA without gam protection, and linear DNA with gam protection. Plasmid DNA used is pBEST-OR2-OR1-Pr-UTR1-deGFP-T500, linear DNA is an 810 bp PCR product with no steric protection ends, and each is supplied at 16 nM. b) Endpoint deGFP expression after 8 hours of 2 nM of linear DNA plotted against signal for different working concentrations of lambda gam, without prior incubation of the protein with crude extract. c) Endpoint deGFP expression from plasmid and linear DNA with or without lambda gam protein, at increasing DNA concentrations. Correlation of 0.98 on plasmid DNA is for 0 nM – 4 nM values only; correlation of 0.99 on linear DNA is for 0 nM – 16 nM. d) Protection of 2 nM of linear DNA using different amounts of non-coding DNA at template ends. Each length corresponds to an amount of non-coding base pairs at each end of the linear DNA, and Sequence 1 is independent of Sequence 2. Readout is endpoint deGFP fluorescence after 8 hours, and experiment is in the presence of lambda gam protein. Error bars represent one standard deviation from three independent experiments.

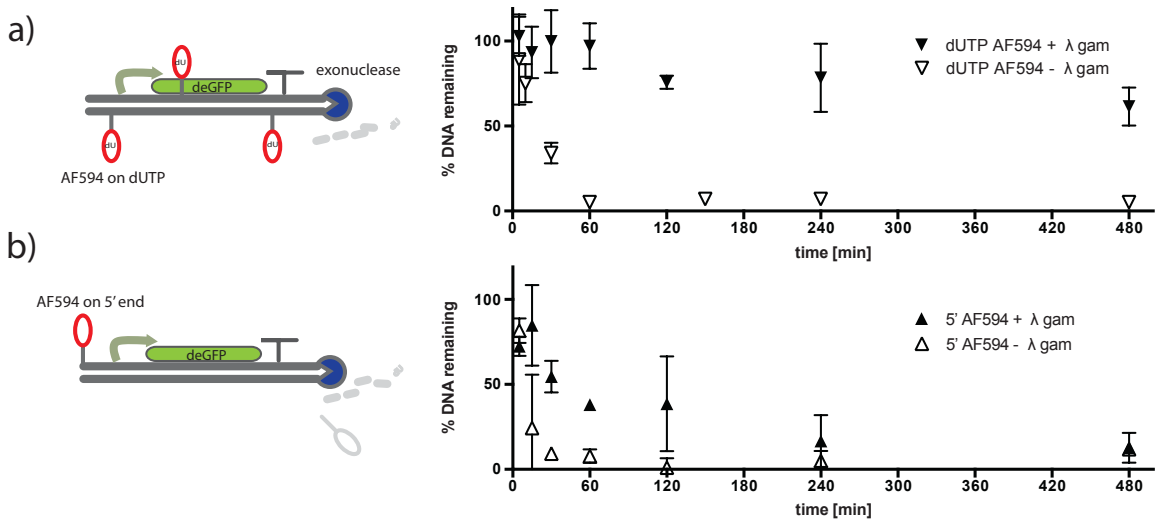

Figure 3. Time-series of DNA degradation in TX-TL at typical working concentrations. a) DNA degradation of 2 nM (25 ng) of DNA with or without 3.5 μM of lambda gam. DNA is labeled throughout by an AlexaFluor-594-5-dUTP incorporated by PCR. Percentage of DNA remaining is based on 25 ng present at time 0. b) Same experiment as panel a), but with AlexaFluor-594 incorporated at the 5' end on a PCR primer. Error bars represent one standard deviation from three independent experiments.

Linear DNA is an alternative for plasmid DNA for circuit prototyping

Although linear DNA provides the fastest method of prototyping circuits, recent studies in other S30 extracts demonstrate a discrepancy between relative expression of linear templates versus plasmid templates [22]. These discrepancies were attributed to structural differences between plasmid and linear DNA, as relative activity was recovered by re-ligation of linear DNA and was independent of translation. We hypothesized that despite structural differences between linear and plasmid DNA, prototyping could still be accomplished by calibrating promoter strength based on DNA concentration between linear and plasmid DNA for constitutive promoters. While a large amount of DNA is needed to obtain signal in other kits, TX-TL uniquely allows significant expression for small template concentrations. By working in a linear regime, circuits can be executed such that large amounts of free polymerases and ribosomes exist at all times (Figure S5).

We tested twelve commonly used sigma-70 based promoters and a negative control of random DNA for *in vitro* plasmid strength, *in vitro* linear DNA strength, and *in vivo* strength. Linear DNA was protected with lambda gam protein and 250 bp of non-coding DNA on either end. Nine promoters are minimal sigma-70 promoters from the Biobrick parts library (http://parts.igem.org/), while three are inducible and well-characterized [28, 29]. These constructs all identically express deGFP downstream of an untranslated region containing a strong RBS named "UTR1" [16]. When each Biobrick promoter was compared in the linear regime and normalized to J23101, results *in vivo* followed the relative pattern of plasmid DNA results in TX-TL despite significant expression magnitude differences (Figure 4a). However, results *in vivo* did not correlate strongly to linear DNA results in TX-TL. These findings mirror those done with a similar panel, albeit using a different reporter and a weaker RBS in a separate S30 extract [22]. Each inducible promoter was also tested constitutively with repressor inactivated or not present, and a similar lack of correlation was found between *in vivo* results and TX-TL results for linear DNA (Figure 4b). Interestingly, inducible promoters seemed to have vastly stronger strength relative to the minimal sigma-70 based promoter panel in TX-TL. The same analysis was conducted using concentrations in the saturating regime and differences in expression magnitude in promoters J23151 and OR2-OR1-Pr were observed (Figure S8). We believe this difference is an artifact of comparing promoters in different saturation regimes, and highlights the importance of quantifying DNA concentration to ensure work in a linear regime. Traditionally, previous studies have ignored DNA concentration due to an emphasis on protein expression or due to low extract potency.

For the Pl-tetO1 and Pl-lacO1 promoter, we also characterized the response in TX-TL of linear and plasmid DNA to varying amounts of inducer in the presence of repressor (Figure 4c). Data was fit to a Hill function with a constant Hill coefficient (Supplemental S3). Operator binding dynamics were similar, with a Michelis-Menten binding coefficient within two standard deviations for Pl-tetO1 and within one standard deviation for Pl-lacO1. Data for Pl-tetO1 may be biased, however, as TX-TL showed toxicity at values above 10 μM aTc, which seemed to be below saturation phase. We assumed that for Pl-tetO1 and Pl-lacO1, repression binding and unbinding was similar for linear and plasmid DNA at individual operator site.

To calibrate linear DNA to plasmid DNA for constitutive expression, we tested each promoter at

different concentrations. Based on the results of endpoint expression, a saturation curve can be produced for both linear and plasmid DNA, where expression is plotted as a function of DNA concentration (Figure 4d). We used a cutoff of $r^2 > 0.975$ to determine a linear regime for each promoter (Figure S9). This data was used to develop a calibration table for linear and plasmid DNA, where the slope of the linear regression line indicates promoter strength in the linear regime (Table 1). A Plasmid:Linear (P:L) ratio can also be determined. All promoters were stronger on plasmid DNA than linear DNA, ranging from 1.40-23.74 fold. The carrying capacity of TX-TL was capped at 26000 rfu. However, independent of promoter strength all constructs were in a saturating regime at 32 nM of linear DNA. This indicates that while linear DNA concentrations can be increased to compensate for lower signal, there is a theoretical limit independent of absolute signal strength.

To demonstrate the ability to prototype circuits using either plasmid or linear DNA, we built a 4-piece genetic switch with two fluorescent outputs, deGFP and deCFP (Figure 5) [30]. Linear DNA constructs were derived from plasmid DNA from PCR with 250 bp of steric protection and lambda gam present. 2 nM of each reporter and 1 nM of each repressor were used. We then examined the dynamics of the genetic switch by plotting the endpoint expression values at 36 different combinations of IPTG and aTc inducers. When both deGFP and deCFP are scaled for equivalent expression, the genetic switch behaves as expected with deGFP expression at high IPTG and deCFP expression at high aTc. As predicted, expression from linear DNA at similar concentrations was also lower than for plasmid DNA. Based on this result, we believe linear DNA prototyping offers a viable way to demonstrate circuit viability.

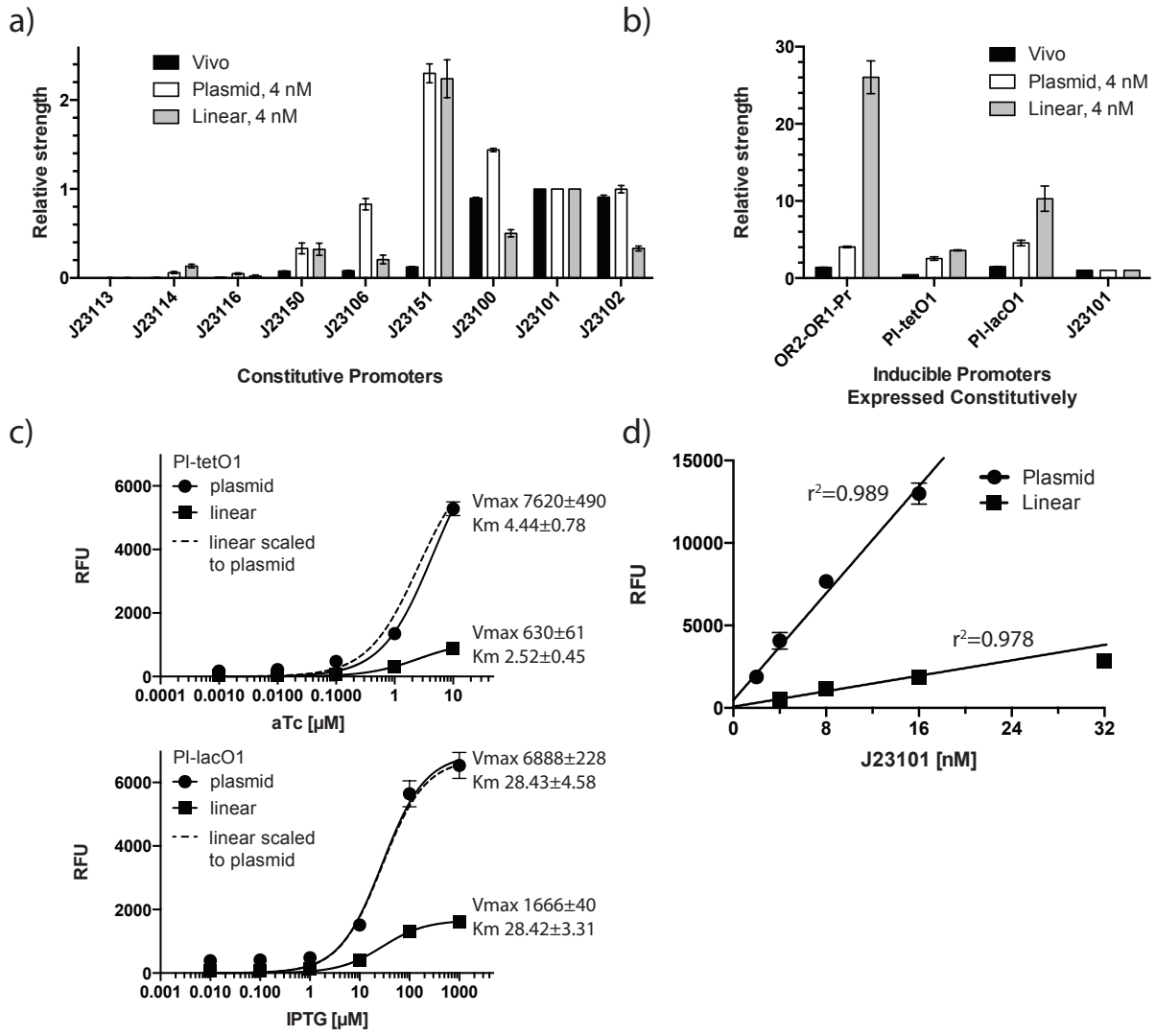

Figure 4. Comparison of different promoter strengths in TX-TL and in vivo. a) Nine commonly used BioBrick promoters were cloned in front of a strong RBS and expressed in either mid-log phase *in vivo*, on plasmids in TX-TL, or on linear DNA pieces in TX-TL. Relative endpoint expression of a 4 nM non-saturating amount of linear and plasmid DNA is scaled to the strength of J23101, with signal from a random promoter sequence subtracted. b) Three inducible promoters expressed constitutively were similarly analyzed, scaled to the strength of J23101. For Pl-lacO1, 0.5 mM of IPTG was added both to the *in vivo* and the TX-TL data to sequester any native lacI repressor. c) Hill functions for Pl-lacO1 and Pl-tetO1 on linear and on plasmid to varying amounts of IPTG and aTc, respectively. 1 nM of a plasmid constitutively producing tetR or lacI is combined with 2 nM of a linear or plasmid reporter. d) Saturation curve for J23101, plotting endpoint fluorescence to concentration of linear or plasmid DNA. Both r^2 and linear regression line are derived from 0 – 16 nM data points. Linear DNA was protected with 250bp of steric protection and with lambda gam. Error bars represent one standard deviation from three independent experiments.

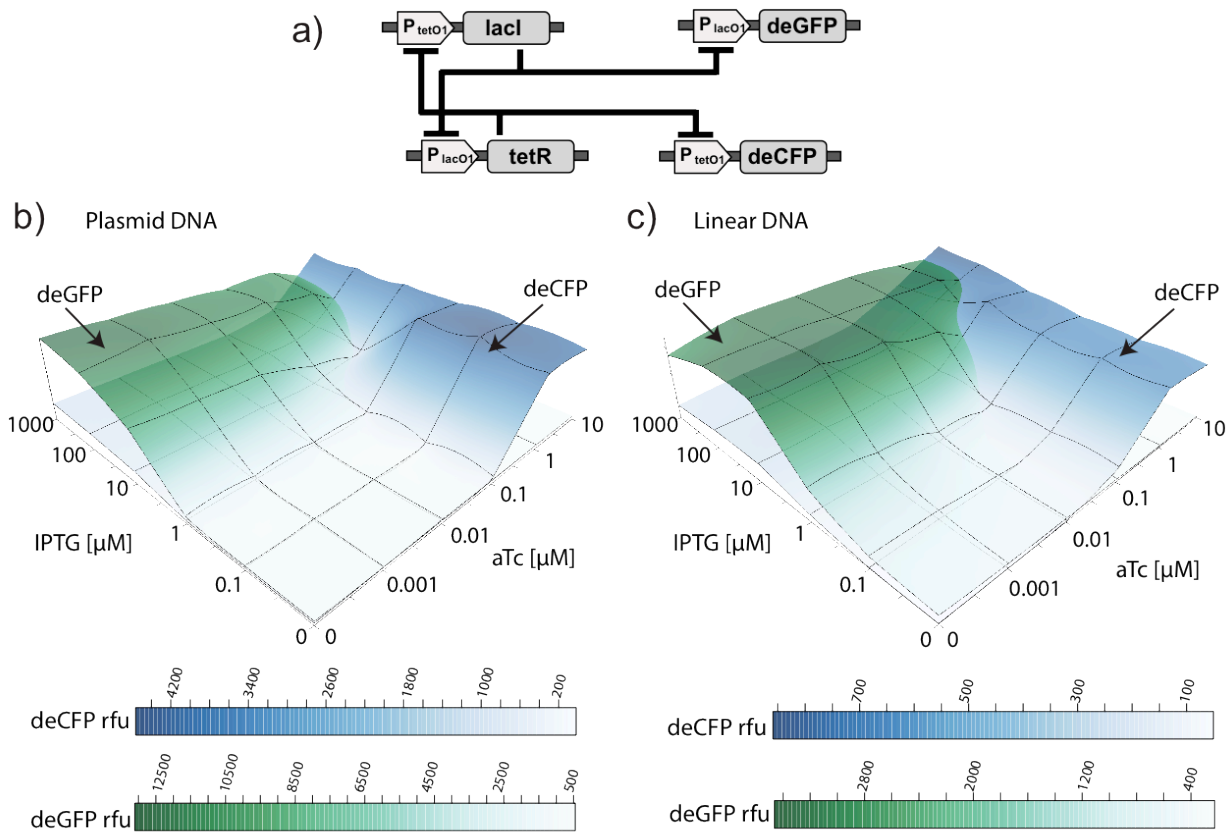

Figure 5. Comparison of a genetic switch made from linear vs. plasmid DNA. a) Diagram of the genetic switch. b) Endpoint fluorescence of deGFP and deCFP for plasmid DNA at various IPTG and aTc inducer concentrations. Four plasmid DNA pieces are used at 2 nM reporter and 1nM repressor. The 0 value is represented as 0.01 μM for IPTG and 0.001 μM for aTc. c) Endpoint fluorescence for four linear DNA pieces at the same concentration. Linear DNA pieces have 250 bp of protection.

Table 1. Calibration data for different promoters in TX-TL. Twelve and one control of random DNA were tested at different concentrations in linear (4-32 nM) and plasmid (2-16 nM) and a linear regime was determined based on a cutoff of $r^2 > 0.975$. The slopes are of the resulting linear regression. P:L ratio is the ratio of the slopes. "nd": signal not detectable, "na": not applicable. Error represents one standard deviation from three independent experiments.

	Plasmid (P)			Linear (L)			
Promoter name	linear regime [DNA] nM	r^2	m	linear regime [DNA] nM	r^2	m	P:L ratio
OR2-OR1-Pr	0-4	0.998	3810 ± 100	0-8	0.979	2726 ± 31.6	1.40
Pl-tetO1	0-8	0.980	2046 ± 49.5	0-16	0.993	392 ± 49.5	5.22
Pl-lacO1	0-4	0.990	4594 ± 192	0-8	0.998	1244 ± 146.2	3.69
J23113	nd	na	na	0-8	0.976	5.4 ± 0.6	na
J23114	0-16	0.985	42.9 ± 1.8	0-16	0.981	20.3 ± 0.4	2.11
J23116	0-16	0.975	37.7 ± 1.9	0-16	0.984	6.1 ± 0.6	6.18
J23150	0-16	0.986	322 ± 16.1	0-16	0.982	38.2 ± 2.0	8.43
J23106	0-8	0.992	724 ± 12.9	0-16	0.996	30.5 ± 1.1	23.74
J23151	0-8	0.982	1879 ± 186	0-8	0.995	321 ± 28.8	5.85
J23100	0-8	0.995	1311 ± 84.4	0-8	0.998	70.8 ± 9.7	18.52
J23101	0-16	0.989	810 ± 30.0	0-16	0.978	117 ± 9.3	6.92
J23102	0-16	0.976	685 ± 31.0	0-16	0.986	41.9 ± 4.4	16.35

Linear DNA can be rapidly assembled for prototyping circuits

After establishing the ability to prototype circuits on linear DNA, we sought to create a rapid assembly method that could assemble and test linear TX-TL ready-pieces in 4-8 hours. The assembly method also must be versatile enough to allow simultaneous transformation to yield plasmid DNA (Figure 6a). Unlike other *in vivo* assembly methods, which ultimately require efficiency as well as selectivity, we are primarily concerned with selectivity as our templates would be end amplified by PCR. We also favored rapid cycle times in linear DNA to modularity post-construction, which has been shown to speed up the design cycle *in vivo* [31]. We initially tested three methods of *in vivo* assembly for adoption purely *in vitro*: Isothermal assembly, Chain Reaction Cloning, and Golden Gate assembly [2, 32, 33]. Each method is based on a different mechanism of action – recombination-based cloning, blunt-end cloning, or sticky-end cloning. Of these three, only Isothermal assembly and Golden Gate assembly produced enough yield to obtain constructs.

We first assembled a common network motif, a negatively autoregulated gene [34], from 4 linear parts using both Isothermal assembly and Golden Gate assembly (Figure S10a). The assembly products were PCR amplified directly afterwards to produce rapid assembly products ready for prototyping in TX-TL. The assembly product was also transformed, cultured, purified, and amplified by PCR to produce a positive control. All constructs were sequenced before testing in TX-TL. When run on an agarose gel, rapid assembly products were of the expected size when compared to a post-transformation positive control, with higher than 95% purity (Figure S10b). However, only certain constructs showed the expected response to aTc inducer (Figure S10c). We determined that non-specific binding products could significantly bias results. To counteract this, we developed a standard assembly procedure based on Golden Gate assembly.

Our standard Golden Gate assembly procedure allowed us to recycle commonly used parts and to ensure functional activity of the desired product. Our standard consists of five pieces – a promoter, 5' untranslated region (UTR), coding sequence, terminator, and vector (Figure S11). It was also designed to be compatible with previously used non-coding sequences and primers on the pBEST vector backbone. We revised a pre-existing standard for use in TX-TL by creating 4 bp binding overhangs with increased specificity [35]. Using different overhangs with little overlap was necessary for adaptation in TX-TL, as we found decreased specificity with multiple base pair overlaps. We also designed our PCR primers to overlap at the junction sites of vector and promoter and vector and terminator, respectively, which further minimized non-specific products. This decreased steric protection ends to 31 bp. We used parts in this standard for subsequent rapid assembly and prototyping.

Using our standard with pre-made pieces, we were able to rapidly prototype a Pl-tetO1-deGFP construct and demonstrate functional equivalency in less than 5 hours (Figure 6b-c). We also wrote a detailed time frame with comparisons to testing using plasmids post-transformation (Table S2). While the assembly reaction did not produce significant amounts of plasmid, a fragment corresponding to the expected size could be amplified. Cleaner products after PCR of assembly reaction were produced by minimizing template concentration and by using overlapping PCR primers (Figure S12). Existing non-specific products could also be predicted based on size and gel mobility shifts. We have since tested multiple assemblies using our rapid

assembly standard, and found that correct equimolar ratios of starting products are also essential to isolating a relatively clonal product. Decreased signal strength of rapid assembly products due to nonspecific products can be compensated for by corresponding increases in DNA concentration.

For more complex circuits, we verified our rapid assembly procedure by repeating the construction of the genetic switch in Figure 5a, but from rapid assembly products (Figure S13a). Specific bands were formed from PCR off of the rapid assembly product, and TX-TL runs demonstrated similar results for the product and the positive control when responding to IPTG and aTc (Figure S13b-c). This prototyping took under 7 hours' time.

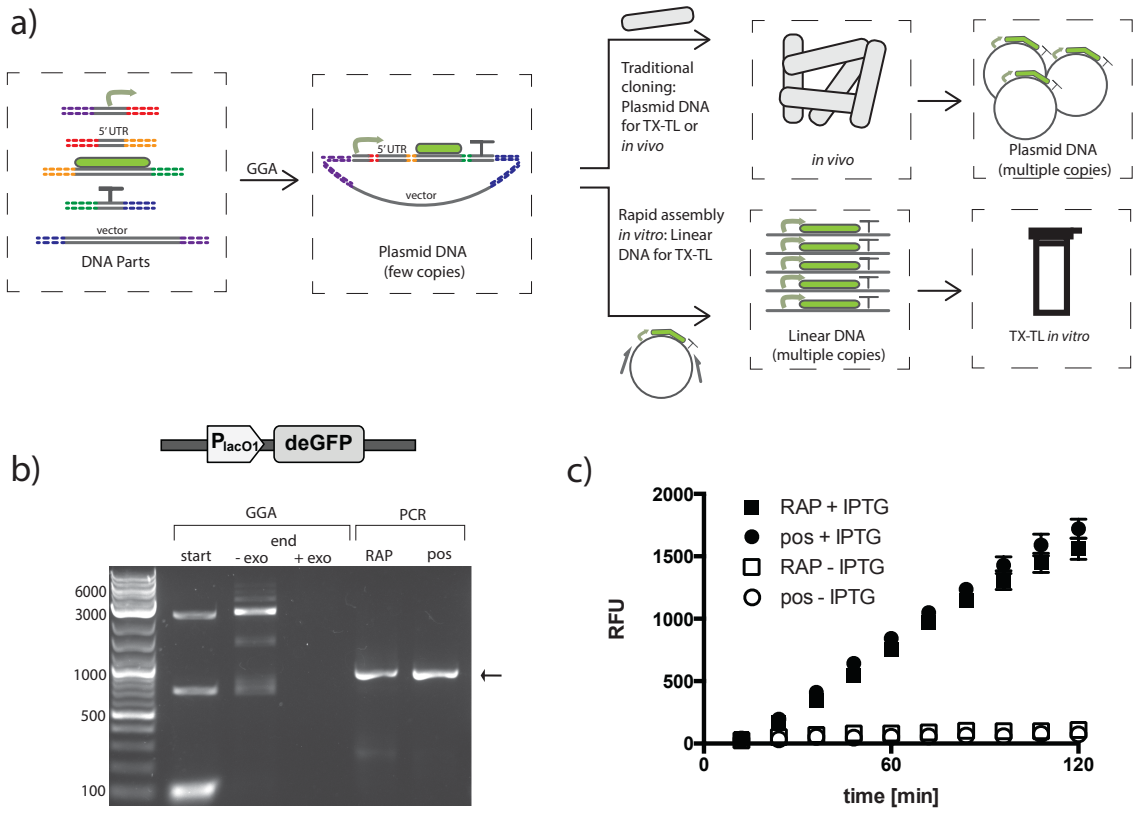

Figure 6. Rapid *in vitro* assembly and prototyping in TX-TL. a) Overview of the rapid assembly and prototyping procedure, where DNA parts are assembled using Golden Gate assembly ("GGA") to create a plasmid, which is then directly used as a PCR template to create linear DNA at high concentrations suitable for TX-TL. In parallel, the assembly product can also be propagated *in vivo* to yield more copies of clonal plasmid. Time comparisons for both methods can be found in Table S2. b) Agarose gel from gene assembled from 5 standard pieces of 66 bp, 103 bp, 110 bp, 707 bp, and 2376 bp. Shown are 50 ng each of starting fragments (except 66 bp), fragments post-assembly before and after exonuclease digestion ("exo"), and rapid assembly PCR product ("RAP") compared to post-cloned PCR product ("pos"). Arrow indicates expected size of 892 bp. c) Functional testing of 4 nM of rapid assembly or post-cloned products, with or without 0.5 mM IPTG inducer. Experiment conducted in the presence of 2 nM Pl-tetO1-lacI linear DNA. Error bars represent one standard deviation from three independent experiments.

Linear DNA prototyping theoretically allows for large circuits to be tested in a single business day

Our work is primarily focused on the technology development of a rapid prototyping procedure using linear DNA in TX-TL. Therefore, we chose only to demonstrate proof-of-concept assemblies using simple circuits. However, the real return of linear DNA prototyping is in testing large circuits in TX-TL. Unlike traditional testing methods reliant on plasmids, the 4-8 hour benchmark provided by our method is theoretically independent of the number of components tested. For example, to initially test an *n*-piece circuit *in vivo* would require $\log_3(n)$ rounds of plasmid cloning, assuming assemblies of 5 units at the same time (four regulatory units plus a vector backbone) (Figure 7a-b). This restriction results from the carrying capacity of the cell to maintain a limited number of antibiotic cassettes and origins of replication. However, an initial testing cycle in TX-TL on linear DNA would require only the theoretical 8 hours, as each construct can be assembled in parallel on linear DNA and immediately tested (Figure 7c). The only restriction would be the resource carrying capacity of the TX-TL reaction. However, large-scale circuit prototyping is limited by the current lack of relatively large synthetic circuits; to our knowledge, the largest currently published circuit is an 11-piece logic gate [36]. Once rapid assembly is established, a larger bottleneck may be the difficulty of formulating and testing novel synthetic circuits with useful function.

To hit the theoretical 8-hour limit for large circuits, the rapid assembly procedure can be automated using robotics with simple pipetting and thermo-cycling capability, as the assemblies rely on standard parts, the final part is PCR amplified, and the resulting part is added to a constant-temperature TX-TL reaction. Unlike traditional methods of testing circuits, there is no cell growth, plasmid minipreps or centrifugation steps.

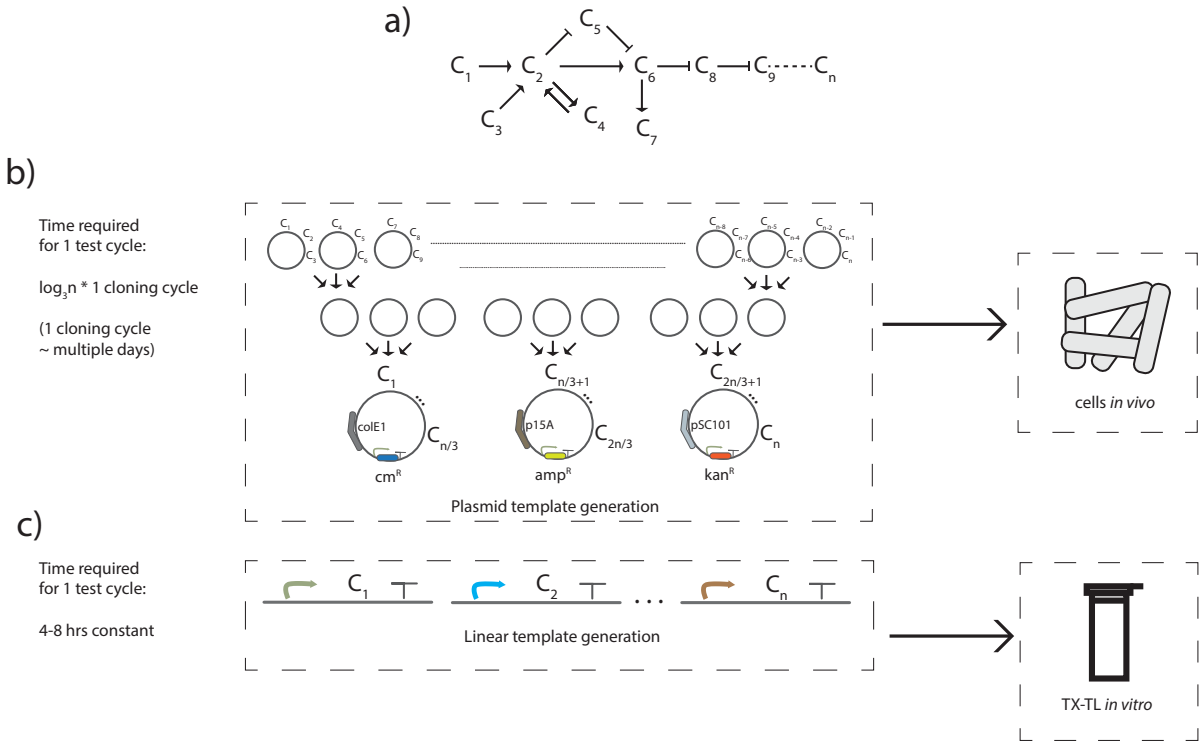

Figure 7. Linear DNA prototyping of large synthetic circuits in TX-TL. a) A large circuit composed of *n* components is to be prototyped *in vivo* or in TX-TL. b) Prototyping *in vivo* requires the reduction of n components to 3 plasmids, which can then be transformed to a cell. c) Prototyping using rapid assembly of linear DNA requires a constant 4-8 hours, as each component can be assembled and tested in parallel.

Conclusion

In this paper, we described a rapid prototyping procedure for genetic circuits through linear DNA in an *E. coli* TX-TL cell-free system. This was done by characterizing methods of protecting linear DNA, and differences in gene expression between linear and plasmid DNA templates. A rapid assembly procedure entirely *in vitro* was developed, which produced results from standard parts in under 8 hours. For a genetic switch, circuits on linear DNA qualitatively match circuits on plasmid DNA. We emphasize using TX-TL on linear DNA to serve as a biomolecular breadboard that can decrease cycle times and complexity and increase iteration speed.

While theoretically linear DNA results can be mapped to plasmid DNA results for more complex circuits, we found that doing so would be unnecessary in our case where only differences in expression amount were observed. Also, in our experience many circuits undergoing prototyping at the initial stages of development do not need the precision that mapping results would provide, as the initial readout is "on" or "off." However, mapping of linear DNA to plasmid DNA results can be theoretically added to computational toolboxes [37].

Although we show in this work that plasmids can be benchmarked to *in vivo* data, we have not focused on moving from TX-TL to *in vivo* for novel circuits. More work needs to be done to characterize differences between circuits run in TX-TL on both linear and plasmid DNA and *in vivo*. For example, for expression off of plasmids we have noticed unexplained expression differences dependent on strain, as well as unexplained linear DNA expression differences between samples that are not processed in parallel. Part of the difference is explained by exogenous steps, such as salt content post-miniprep using different columns [14]. We hypothesize other differences may be intrinsic to the DNA used, either through biochemical modifications or through structural differences which have been shown *in vivo* to affect gene expression [38]. While we try to compensate by collecting samples per experiment in one batch using the same processing techniques, a better understanding of the contributors to experimental variation in TX-TL is necessary. However, rapid prototyping as part of a biological breadboard should be a useful concept for any future work using TX-TL for synthetic circuit design, with an emphasis on novel complex circuits.

Supporting Information Available: Supporting information includes additional text, tables, and figures referenced in this article. This material is available free of charge via the Internet at http://pubs.acs.org.

METHODS:

Cell-free expression preparation and execution:
Preparation of the cell-free TX-TL expression system was done according to previously described protocols, resulting in extract with conditions: 8.9-9.9 mg/mL protein, 4.5 mM-10.5 mM Mg-glutamate, 40-160 mM K-glutamate, 0.33-3.33 mM DTT, 1.5 mM each amino acid except leucine, 1.25 mM leucine, 50 mM HEPES, 1.5 mM ATP and GTP, 0.9 mM CTP and UTP, 0.2 mg/mL tRNA, 0.26 mM CoA, 0.33 mM NAD, 0.75 mM cAMP, 0.068 mM folinic acid, 1 mM spermidine, 30 mM 3-PGA, 2% PEG-8000 [14]. Unless otherwise specified, one extract set "eZS1" is used consistently throughout the experiments to prevent variation from batch to batch. Extract "e10" was similarly prepared for toxicity assays. Extract "e13" was prepared using above conditions, but grew only at 29°C with a 12-hour second incubation. TX-TL reactions are conducted in a volume of 10 µL in a 384-well plate (Nunc) at 29°C, using a three tube system: extract, buffer, and DNA. When possible, inducers such as IPTG or purified proteins such as lambda gam were added to a mix of extract and buffer to ensure uniform distribution. For deGFP, samples were read in a Synergy H1 plate reader (Biotek) using settings for excitation/emission: 485 nm/ 525 nm, gain 61. For deCFP, settings were: 440 nm/ 480 nm, gain 61. All samples were read in the same plate reader; therefore, rfu units should be considered equivalent in magnitude for each reporter. Unless otherwise stated, endpoint measurements are presented after 8 hours of expression at 29°C.

Lambda gam protein purification:
The composition of buffers used is as follows: Buffer L: 50 mM Tris-Cl pH 8, 500 mM NaCl, 5mM imidazole, 0.1% Triton X; buffer W: 50 mM Tris-Cl pH 8, 500 mM NaCl, 25 mM imidazole; buffer E: 50 mM Tris-Cl pH 8, 500 mM NaCl, 250 mM imidazole; buffer S: 50 mM Tris-Cl pH 7.5, 100mM NaCl, 1mM DTT, 1mM EDTA, 2% DMSO. A frozen stock of P_araBAD-gamS in a BL21-DE3 *E. coli* strain was grown overnight in LB-carbenicillin media. 100 mL was used to inoculate 1 L LB-carbenicillin to an OD 600 nm of 0.4-0.6 at 37°C, 220 rpm. Cells were then incubated to 0.25% arabinose (final concentration) and grown for four additional hours at 25 C, 220 rpm, before being pelleted and frozen at -80°C. Cells were resuspended in buffer L, mechanically lysed, and incubated with Ni-NTA agarose (Qiagen). Ni-NTA agarose was washed twice with 15 column volumes of buffer W and eluted in buffer E. Fractions with a ~13 kD band were concentrated and dialyzed into buffer S overnight, and further purified on a 26/60 Sephadex 75 column. Protein concentration was verified by Bradford, concentrated to 3 mg/ml using an Ultra-0.5 3K MWCO Centrifugal Filter (Ambion), and stored in buffer S at -80°C. Protein purity was verified by gel. Purification steps were verified by SDS-PAGE gel electrophoresis.

Plasmid DNA and PCR product preparation:
Plasmids used in this study were constructed using standard cloning procedures and maintained in a KL740 strain if using an OR2-OR1 promoter (29°C), a MG1655Z1 strain if using a Pl-tetO1 or Pl-lacO1 promoter, a BL21-DE3 strain for protein purification, a BL21 strain for promoter characterization, or a JM109 strain for all other constructs. KL740 upregulates a temperature sensitive lambda cI repressor, and MG1655Z1 upregulates tetR and lacI. PCR products are

amplified using Pfu Phusion Polymerase (New England Biolabs) for all constructs except for those labeled with AlexaFluor-588-5-dUTP, which used Taq Polymerase (New England Biolabs), and were DpnI digested. Plasmids were either miniprepped using a PureYield column (Promega) or midiprepped a NucleoBond Xtra Midi column (Macherey-Nagel). All plasmids were processed at stationery phase. Before use in the cell-free reaction, both plasmids and PCR products undergo an additional PCR purification step using a QiaQuick column (Qiagen) which removes excess salt detrimental to TX-TL, and are eluted and stored in 10mM Tris-Cl solution, pH 8.5 at 4°C for short term storage and -20°C for long term storage.

Sequences used for steric protection:
Three sets of sequences were used for steric protection assays. One set was based on the vector backbone of previously published pBEST-OR2-OR1-Pr-UTR1-deGFP-T500 (Addgene #40019). Another set, used only in Figure 2d and referred to as "Sequence 2", was derived from the coding sequence of *gltB* and *lhr*. These sequences were found by parsing the NCBI GenBank MG1655 record in BioPython for all known coding sequences and sorting by size. A final set, used in Figure 4, was based on the vector backbone of pBEST-p15A-OR2-OR1-Pr-UTR1-deGFP-T500. Sequences were analyzed using Geneious 6.0 (Biomatters Ltd).

In vitro linear DNA assembly:
Linear DNA fragments are amplified using Pfu Phusion Polymerase (New England Biolabs), DpnI digested for 5 minutes at 37°C (New England Biolabs) while verified with agarose gel electrophoresis, and PCR purified using previously described procedures. Fragments are then assembled *in vitro* using either Isothermal Assembly or Golden Gate Assembly. For Isothermal Assembly, Gibson Assembly Master Mix (New England Biolabs) was used according to manufacturer instructions with 1:3 molar ratio vector:insert, and reacted at 1 hour at 50°C [2]. For Golden Gate Assembly, a 15 μL reaction was set up consisting of equimolar amounts of vector and insert, 1.5 μL 10x NEB T4 Buffer (New England Biolabs), 1.5 μL 10x BSA (New England Biolabs), 1 μL BsaI (New England Biolabs), and 1 μL T4 Ligase at 2 million units/mL (New England Biolabs) [33]. Reactions were run in a thermocycler at: 10 cycles of 2min/37°C, 3min/20°C, 1 cycle 5min/50°C, 5min/80°C. For Golden Gate Assembly, constructs with internal BsaI cut sites were silently mutated beforehand using a QuikChange Lightning Multi Site-Directed Mutagenesis Kit (Agilent). 1 μL of the resulting assembly product is PCR amplified for 35 cycles in a 50 μL PCR reaction, and verified by agarose gel electrophoresis. If the resulting band is 80% or more pure, the resulting DNA is PCR purified using previously described procedures and used directly in TX-TL. Simultaneously, 2 μL of the assembly product is transformed into cells using standard chemically competent or electrically competent procedures, grown, miniprepped, and sequenced. For the Lambda Exonuclease / Exonuclease digest assay, we followed the assembly procedure up to assembly completion but using twice the amount of assembly mix. Then, a 20 μL reaction was prepared with 12 μL assembly product, 2 μL 10x ExoI reaction buffer (New England Biolabs), 2 μL 10x BSA (New England Biolabs), 0.5 μL Lambda Exonuclease (New England Biolabs), 0.5 μL Exonuclease I (New England Biolabs), and 3 μL water. The control was not digested. Reaction was run for 1 hour at 37°C and PCR purified using previously described procedures.

Linear DNA degradation assay:
To form linear DNA with AlexaFluor distributed on the dUTP, template DNA producing deGFP

was amplified using a Taq Polymerase (New England Biolabs) and AlexaFluor-594-5-dUTP (Invitrogen) according to manufacturer standards with a 1:3:4:4:4 ratio of AlexaFluor-5-dUTP:dTTP:dCTP:dATP:dGTP (New England Biolabs), DpnI digested, and PCR purified using previously described procedures. Successful labeling was verified through comparison of pre-stained and SybrSafe post-stained agarose gel electrophoresis (Invitrogen). To form linear DNA with AlexaFluor on the 5' end, AlexaFluor 594 was covalently linked on the 5' end to both forward and reverse synthetic primers (Integrated DNA Technologies) and used for PCR amplificaton. For the 2 nM assay, DNA was then added to a 105 μL TX-TL reaction in triplicate with or without lambda gam protein, and incubated at 29°C. A negative control with no DNA was done in parallel. Aliquots of 10 μL were removed at indicated time points and immediately added to 50 μL of PB buffer (Qiagen) and flash-frozen in LN2. In parallel, 2 μL of sample was read for deGFP fluorescence on a Synergy H1 Take3 Plate (Biotek). After all samples were collected, samples were PCR-purified to remove degraded components and measured on a 384-well plate (Nunc) using setting excitation/emission: 590 nm/617 nm, gain 100. Negative control values were subtracted per data point. GFP signal was normalized to endpoint fluorescence and AlexaFluor-594 signal was normalized to DNA present at time 0. For the 250 ng assay, similar procedures were followed except 20 nM of DNA was added to 40 μL TX-TL reactions for teach condition in triplicate and aliquots of 5 μL were removed and added to 25 μL of PB buffer (Qiagen).

In vivo promoter characterization:

Twelve promoters and a random control sequence of DNA were cloned in front of UTR1-deGFP-T500 on a p15A low copy plasmid using standard cloning procedures and propagated at 29°C in BL21 *E. coli* (New England Biolabs). Growth at 37°C or cloning on a high-copy colE1 plasmid resulted in a significant mutation rate. Single colonies were simultaneously sequenced and mixed with glycerol for storage at -80°C. Specific sequences can be found in Supplemental S2. Frozen stocks were used to inoculate 300 mL of culture in MOPS-glycerol-carbenicillin media (MOPS EZ Rich Defined Medium Kit, Teknova, using 0.4% glycerol working concentration in lieu of glucose and adding 100 μg/ml of carbenicillin) in a 96 DeepWell polypropylene plate (Fisher Scientific). The Pl-lacO1 sample was grown with 0.5mM of IPTG in addition. Plate was covered with a BreatheEasy gas-permeable membrane (Sigma-Aldrich) and grown overnight at 29°C on a Symphony Incubating Microplate Shaker (VWR), shaking at 900 rpm. Cultures were then diluted 1:50 in triplicate, grown for 4 hours at 29°C, and diluted to an OD 600 nm of 0.1 – 0.2 in triplicate depending on growth rate. Cultures were then grown for 90 minutes at 29°C, and transferred to a CulturPlate 96-well plate (PerkinElmer) for OD 600 nm and fluorescent measurement at excitation/emission 485 nm/520 nm on a Synergy H1 plate reader (Biotek). Background fluorescence from media was subtracted, and each sample was normalized to OD 600 nm. The normalized value for the random control was then subtracted. Each sample was then normalized to J23101.

TX-TL promoter characterization on linear and plasmid DNA:

Sequenced cultures from frozen stocks were used to inoculate 20 mL of LB-carbenicillin media and grown in parallel to stationery phase. For each sample, 4 x 3 mL of sample were

miniprepped using previously described procedures. The miniprep products were PCR purified into one 30 μL sample, and re-sequenced. To generate linear DNA for each sample with 250 bp of non-coding DNA at each end, the resulting plasmid was PCR amplified in 4 x 50 μL reactions, DpnI digested, and PCR purified into one 30 μL sample. Plasmid and linear DNA were quantified by spectrophotometry. For each promoter, DNA was diluted 1:2 from 4-32 nM for linear DNA or 2–6 nM for plasmid DNA in water or 0.5 mM IPTG for Pl-lacO1. To generate relative strength to J23101, background fluorescence and random control sequence fluorescence was subtracted per promoter sample, and endpoint data was normalized to J23101. To generate saturation curves, background fluorescence was subtracted per promoter sample, and correlation and slope for each promoter (including the random control sequence) was determined.

TX-TL promoter induction curves:

DNA was prepared as previously mentioned. For Pl-lacO1, 1 nM of a Pl-tetO1-lacI plasmid and 2 nM of either linear or plasmid Pl-lacO1-deGFP were combined with varying amounts of IPTG in the presence of lambda gam and endpoint fluorescence was read. For Pl-tetO1, the same was done but with 1 nM of a Pl-lacO1-tetR plasmid, 2nM of either linear or plasmid Pl-tetO1-deGFP, and 0.5 mM of IPTG in addition to aTc and lambda gam to inactivate any lacI present in the extract. Data was subtracted from background fluorescence for those containing aTc.

ACKNOWLEDGEMENTS:

We thank Shaobin Guo, Dan Siegal-Gaskins, Anu Thubagere, Jongmin Kim, and Patrik Lundin for assistance testing initial methods of linear DNA assembly and protection, Emmanuel de Los Santos for advice on protein purification, Victoria Hsiao for assistance on *in vivo* assays, Angela Ho and Jost Vielmetter for protein purification through the Caltech Protein Expression Center and contribution of Figure S3a, and Clare Chen and Barclay Lee for assistance in the early stages of the project. This material is based upon work supported in part by the Defense Advanced Research Projects Agency (DARPA/MTO) Living Foundries program, contract number HR0011-12-C-0065 (DARPA/CMO). Z.Z.S. is also supported by a UCLA/Caltech Medical Scientist Training Program fellowship and Z.Z.S and E.Y are supported by National Defense Science and Engineering Graduate fellowships. The views and conclusions contained in this document are those of the authors and should not be interpreted as representing officially policies, either expressly or implied, of the Defense Advanced Research Projects Agency or the U.S. Government.

AUTHOR CONTRIBUTIONS:

Z.Z.S., E.Y., and C.A.H., designed the experiments with guidance from V.N and R.M.M. Z.Z.S performed the experiments. All analyzed the data. Z.Z.S and E.Y. wrote the manuscript. The authors declare no competing financial interest.

References:

1. Green, M.R., J. Sambrook, and J. Sambrook, *Molecular cloning : a laboratory manual*. 4th ed. 2012, Cold Spring Harbor, N.Y.: Cold Spring Harbor Laboratory Press.
2. Gibson, D.G., et al., *Enzymatic assembly of DNA molecules up to several hundred kilobases.* Nat Methods, 2009. **6**(5): p. 343-5.
3. Alzari, P.M., et al., *Implementation of semi-automated cloning and prokaryotic expression screening: the impact of SPINE.* Acta Crystallogr D Biol Crystallogr, 2006. **62**(Pt 10): p. 1103-13.
4. Ro, D.K., et al., *Production of the antimalarial drug precursor artemisinic acid in engineered yeast.* Nature, 2006. **440**(7086): p. 940-3.
5. Kwok, R., *Five hard truths for synthetic biology.* Nature, 2010. **463**(7279): p. 288-90.
6. Forster, A.C. and G.M. Church, *Synthetic biology projects in vitro.* Genome Research, 2007. **17**(1): p. 1-6.
7. Noireaux, V., R. Bar-Ziv, and A. Libchaber, *Principles of cell-free genetic circuit assembly.* Proceedings of the National Academy of Sciences of the United States of America, 2003. **100**(22): p. 12672-12677.
8. Hockenberry, A.J. and M.C. Jewett, *Synthetic in vitro circuits.* Curr Opin Chem Biol, 2012. **16**(3-4): p. 253-9.
9. Kim, J., K.S. White, and E. Winfree, *Construction of an in vitro bistable circuit from synthetic transcriptional switches.* Mol Syst Biol, 2006. **2**: p. 68.
10. Kim, J. and E. Winfree, *Synthetic in vitro transcriptional oscillators.* Mol Syst Biol, 2011. **7**: p. 465.
11. Saito, H., et al., *Synthetic translational regulation by an L7Ae-kink-turn RNP switch.* Nat Chem Biol, 2010. **6**(1): p. 71-8.
12. Shimizu, Y., et al., *Cell-free translation reconstituted with purified components.* Nature Biotechnology, 2001. **19**(8): p. 751-755.
13. Nirenberg, M.W. and J.H. Matthaei, *The dependence of cell-free protein synthesis in E. coli upon naturally occurring or synthetic polyribonucleotides.* Proc Natl Acad Sci U S A, 1961. **47**: p. 1588-602.
14. Sun, Z.Z., et al., *Protocols for Implementing an Escherichia Coli Based TX-TL Cell-Free Expression System for Synthetic Biology.* Journal of Visualized Experiments, 2013. **e50762**.
15. Shin, J. and V. Noireaux, *Study of messenger RNA inactivation and protein degradation in an Escherichia coli cell-free expression system.* J Biol Eng, 2010. **4**: p. 9.
16. Shin, J. and V. Noireaux, *Efficient cell-free expression with the endogenous E. Coli RNA polymerase and sigma factor 70.* J Biol Eng, 2010. **4**: p. 8.
17. Karzbrun, E., et al., *Coarse-grained dynamics of protein synthesis in a cell-free system.* Phys Rev Lett, 2011. **106**(4): p. 048104.
18. Shin, J. and V. Noireaux, *An E. coli cell-free expression toolbox: application to synthetic gene circuits and artificial cells.* ACS Synth Biol, 2012. **1**(1): p. 29-41.
19. Shin, J., P. Jardine, and V. Noireaux, *Genome Replication, Synthesis, and Assembly of the Bacteriophage T7 in a Single Cell-Free Reaction.* Acs Synthetic Biology, 2012. **1**(9): p. 408-413.

20. Murphy, K.C., *Lambda Gam protein inhibits the helicase and chi-stimulated recombination activities of Escherichia coli RecBCD enzyme.* J Bacteriol, 1991. **173**(18): p. 5808-21.
21. Sitaraman, K., et al., *A novel cell-free protein synthesis system.* J Biotechnol, 2004. **110**(3): p. 257-63.
22. Chappell, J., K. Jensen, and P.S. Freemont, *Validation of an entirely in vitro approach for rapid prototyping of DNA regulatory elements for synthetic biology.* Nucleic Acids Res, 2013. **41**(5): p. 3471-81.
23. Lin, C.H., Y.C. Chen, and T.M. Pan, *Quantification bias caused by plasmid DNA conformation in quantitative real-time PCR assay.* PLoS One, 2011. **6**(12): p. e29101.
24. Ott, J. and F. Eckstein, *Protection of oligonucleotide primers against degradation by DNA polymerase I.* Biochemistry, 1987. **26**(25): p. 8237-41.
25. Dillingham, M.S. and S.C. Kowalczykowski, *RecBCD enzyme and the repair of double-stranded DNA breaks.* Microbiol Mol Biol Rev, 2008. **72**(4): p. 642-71, Table of Contents.
26. Murphy, K.C., *The lambda Gam protein inhibits RecBCD binding to dsDNA ends.* J Mol Biol, 2007. **371**(1): p. 19-24.
27. Seki, E., et al., *Cell-free protein synthesis system from Escherichia coli cells cultured at decreased temperatures improves productivity by decreasing DNA template degradation.* Anal Biochem, 2008. **377**(2): p. 156-61.
28. Kelly, J.R., et al., *Measuring the activity of BioBrick promoters using an in vivo reference standard.* J Biol Eng, 2009. **3**: p. 4.
29. Lutz, R. and H. Bujard, *Independent and tight regulation of transcriptional units in Escherichia coli via the LacR/O, the TetR/O and AraC/I1-I2 regulatory elements.* Nucleic Acids Res, 1997. **25**(6): p. 1203-10.
30. Gardner, T.S., C.R. Cantor, and J.J. Collins, *Construction of a genetic toggle switch in Escherichia coli.* Nature, 2000. **403**(6767): p. 339-42.
31. Litcofsky, K.D., et al., *Iterative plug-and-play methodology for constructing and modifying synthetic gene networks.* Nat Methods, 2012. **9**(11): p. 1077-80.
32. Pachuk, C.J., et al., *Chain reaction cloning: a one-step method for directional ligation of multiple DNA fragments.* Gene, 2000. **243**(1-2): p. 19-25.
33. Engler, C., R. Kandzia, and S. Marillonnet, *A one pot, one step, precision cloning method with high throughput capability.* PLoS One, 2008. **3**(11): p. e3647.
34. Rosenfeld, N., M.B. Elowitz, and U. Alon, *Negative autoregulation speeds the response times of transcription networks.* J Mol Biol, 2002. **323**(5): p. 785-93.
35. Sarrion-Perdigones, A., et al., *GoldenBraid: an iterative cloning system for standardized assembly of reusable genetic modules.* PLoS One, 2011. **6**(7): p. e21622.
36. Moon, T.S., et al., *Genetic programs constructed from layered logic gates in single cells.* Nature, 2012. **491**(7423): p. 249-53.
37. Tusa, Z.A., et al., *An In Silico Modeling Toolbox for Rapid Prototyping of Circuits in a Biomolecular "Breadboard" System*, in *2013 Conference on Decision and Control*2013, IEEE: Florence, Italy.
38. Higgins, C.F., et al., *A physiological role for DNA supercoiling in the osmotic regulation of gene expression in S. typhimurium and E. coli.* Cell, 1988. **52**(4): p. 569-84.

Supplemental Information for:

Linear DNA for rapid prototyping of synthetic biological circuits in an *Escherichia coli* based TX-TL cell-free system

Zachary Z. Sun, Enoch Yeung, Clarmyra A. Hayes, Vincent Noireaux, Richard M. Murray

Included in this insert are Supplemental S1 – S3, Table S1 – S2, Figures S1 – S13, and Supplemental References.

Supplemental S1.

We required a method to accurately quantify broad ranges of DNA, and tested both spectrophotometry and fluorometry. Both have known advantages and disadvantages: in particular, spectrophotometry is known to be inaccurate at low DNA concentrations, while fluorometry can produce biased plasmid DNA results due to conformational changes [1]. Comparing spectrophotometry (Nanodrop 2000) to fluorometry (Qubit 2.0 dsDNA HS and BR Assay), we found that linear DNA and plasmid DNA were most accurate and precise on the Nanodrop when at concentrations above 30 ng/μL, incurring at most 5.17% error (Figure S1, Table S1). However, for linear DNA from 2-30 ng/μL both of the dsDNA HS and BR Assays had superior accuracy and precision, incurring at most 12.02% error. For plasmid DNA from 2-30 ng/μL only the dsDNA BR Assay using a linear standard was accurate and precise, incurring 5.07% error. Based on these results, for subsequent data we quantified all constructs above 30 ng/μL on the Nanodrop, end-working concentration linear DNA from 2-30 ng/μL using the Qubit dsDNA HS Assay, and end-working concentration plasmid DNA from 2-30 ng/μL either from diluted Nanodrop stocks above 30 ng/μL or using the dsDNA BR Assay.

DNA Quantification Materials and Methods

A Nanodrop 2000 UV-Vis spectrophotometer (Thermo Fisher Scientific) and a Qubit 2.0 fluorometer (Invitrogen) were used to measure dsDNA concentration. Per run, either 500 ng/μL of 1 kb DNA ladder (New England Biolabs) or 500 ng/μL of supercoiled DNA ladder (New England Biolabs) were diluted 1:2 down to 0.98 ng/μL in TE buffer and used as experimental samples. For the Nanodrop, 2 μL of sample was used to determine concentration. For the Qubit, 2 μL of sample was combined with 198 μL of supplied reagent:buffer to determine concentration. Different standards were tested for the Qubit, depending on the assay (dsDNA BR or dsDNA HS) and the type of DNA quantified (linear or plasmid). Linear standards were supplied by the manufacturer; plasmid standards consisted of pUC19 vector at 1000 ng/μL (New England Biolabs) diluted 1:10 in TE for the dsDNA BR assay or 1:100 for the dsDNA HS assay.

Supplemental S2.

The following plasmids, relevant DNA pieces, and primers were used in the study, along with NCBI GenBank Accession IDs and/or Addgene Plasmid Depository Information and sequence data (if applicable).

Plasmids

Name	Short ID	GenBank	Addgene	Notes
pBEST-p15A-Pl-tetO1-UTR1-lacI-T500	1		45784	
pBEST-p15A-Pl-tetO1-UTR1-deGFP-T500	2		45392	
pBEST-p15A-Pl-lacO1-UTR1-TetR-T500	3			
pBEST_OR2-OR1-Pr_UTR1_deCFP_T500	18			
pBEST_OR2-OR1-Pr_UTR1_deGFP-T500	21		40019	
pBADmod1-linker2-gamS	22			
pBEST-colE1-Pl-tetO1-UTR1-deGFP-T500	58			
pBEST-2kblhr2-OR2-OR1-Pr_UTR1_deGFP_T500-1gltB2kb	87			Derived from gltB and lhr genes from NC_000913 cloned into 21, with G->A silent mutation.
pBEST_OR2-OR1-Pr_UTR1-deGFP-T500 BsaI, BbsI-safe	105			Derived from 21 with mutations to make it BsaI, BbsI compatible
pBEST-Pl-tetO1-tetR-linker-deGFP-T500	109			Post cloned 4-piece GGA or Isothermal assembly
pBEST-p15A-Pl-tetO1-UTR1-lacI-T500 BsaI, BbsI-safe	113			
pBEST-p15A-OR2-OR1-Pr-UTR1-deGFP-T500	121			Derived from 1 and insert
pBEST-p15A-Pl-tetO1-deGFP-T500	122			Derived from 1 and insert
pBEST-p15A-Pl-lacO1-deGFP-T500	123			Derived from 1 and insert
pBEST-p15A-J23113-deGFP-T500	124			Derived from 1 and insert
pBEST-p15A-J23114-deGFP-T500	125			Derived from 1 and insert
pBEST-p15A-J23116-deGFP-T500	126			Derived from 1 and insert
pBEST-p15A-J23150-deGFP-T500	127			Derived from 1 and insert
pBEST-p15A-J23106-deGFP-T500	128			Derived from 1 and insert
pBEST-p15A-J23151-deGFP-T500	129			Derived from 1 and insert
pBEST-p15A-J23100-deGFP-T500	130			Derived from 1 and insert
pBEST-p15A-J23101-deGFP-T500	131			Derived from 1 and insert
pBEST-p15A-J23102-deGFP-T500	132			Derived from 1 and insert
pBEST-p15A-pNull-deGFP-T500	133			Derived from 1 and insert
P3U2C7T2-v1-1 (Pl-lacO1-deGFP)	134			Post cloned 5-piece GGA
P4U2C8T2-v1-1 (Pl-tetO1-deCFP)	135			Post cloned 5-piece GGA
P3U2C5T2-v1-2 (Pl-lacO1-tetR)	136			Post cloned 5-piece GGA
P4U2C6T2-v1-2 (Pl-tetO1-lacI)	137			Post cloned 5-piece GGA

Promoters, Regulatory Elements, and Coding Sequences

Name	Sequence
OR2-OR1-Pr	TGAGCTAACACCGTGCGTGTTGACAATTTTACCTCTGGCGGTGATAATGGTT GCA
Pl-tetO1	TCCCTATCAGTGATAGAGATTGACATCCCTATCAGTGATAGAGATACTGAGC ACA
Pl-lacO1	ATAAATGTGAGCGGATAACATTGACATTGTGAGCGGATAACAAGATACTGA GCACA
J23113	CTGATGGCTAGCTCAGTCCTAGGGATTATGCTAGC
J23114	TTTATGGCTAGCTCAGTCCTAGGTACAATGCTAGC
J23116	TTGACAGCTAGCTCAGTCCTAGGGACTATGCTAGC
J23150	TTTACGGCTAGCTCAGTCCTAGGTATTATGCTAGC
J23106	TTTACGGCTAGCTCAGTCCTAGGTATAGTGCTAGC
J23151	TTGATGGCTAGCTCAGTCCTAGGTACAATGCTAGC
J23100	TTGACGGCTAGCTCAGTCCTAGGTACAGTGCTAGC
J23101	TTTACAGCTAGCTCAGTCCTAGGTATTATGCTAGC
J23102	TTGACAGCTAGCTCAGTCCTAGGTACTGTGCTAGC
pNull	ATTCTGGGATTATACAGTAGTAATCACTAATTTAC
UTR1	AATAATTTTGTTTAACTTTAAGAAGGAGATATA
T500	CAAAGCCCGCCGAAAGGCGGGCTTTTCTGT
deGFP	ATGGAGCTTTTCACTGGCGTTGTTCCCATCCTGGTCGAGCTGGACGGCGACG TAAACGGCCACAAGTTCAGCGTGTCCGGCGAGGGCGAGGGCGATGCCACCT ACGGCAAGCTGACCCTGAAGTTCATCTGCACCACCGGCAAGCTGCCCGTGC CCTGGCCCACCCTCGTGACCACCCTGACCTACGGCGTGCAGTGCTTCAGCCG CTACCCCGACCACATGAAGCAGCACGACTTCTTCAAGTCCGCCATGCCCGA AGGCTACGTCCAGGAGCGCACCATCTTCTTCAAGGACGACGGCAACTACAA GACCCGCGCCGAGGTGAAGTTCGAGGGCGACACCCTGGTGAACCGCATCGA GCTGAAGGGCATCGACTTCAAGGAGGACGGCAACATCCTGGGGCACAAGCT GGAGTACAACTACAACAGCCACAACGTCTATATCATGGCCGACAAGCAGAA GAACGGCATCAAGGTGAACTTCAAGATCCGCCACAACATCGAGGACGGCAG CGTGCAGCTCGCCGACCACTACCAGCAGAACACCCCCATCGGCGACGGCCC CGTGCTGCTGCCCGACAACCACTACCTGAGCACCCAGTCCGCCCTGAGCAA AGACCCCAACGAGAAGCGCGATCACATGGTCCTGCTGGAGTTCGTGACCGC CGCCGGGATCTAA
deCFP	ATGGAGCTTTTCACTGGCGTTGTTCCCATCCTGGTCGAGCTGGACGGCGACG TAAACGGCCACAAGTTCAGCGTGTCCGGCGAGGGCGAGGGCGATGCCACCT ACGGCAAGCTGACCCTGAAGTTCATCTGCACCACCGGCAAGCTGCCCGTGC CCTGGCCCACCCTCGTGACCACCCTGACCTGGGGCGTGCAGTGCTTCAGCCG CTACCCCGACCACATGAAGCAGCACGACTTCTTCAAGTCCGCCATGCCCGA AGGCTACGTCCAGGAGCGCACCATCTTCTTCAAGGACGACGGCAACTACAA GACCCGCGCCGAGGTGAAGTTCGAGGGCGACACCCTGGTGAACCGCATCGA GCTGAAGGGCATCGACTTCAAGGAGGACGGCAACATCCTGGGGCACAAGCT GGAGTACAACTACATCAGCCACAACGTCTATATCACCGCCGACAAGCAGAA GAACGGCATCAAGGCCAACTTCAAGATCCGCCACAACATCGAGGACGGCAG CGTGCAGCTCGCCGACCACTACCAGCAGAACACCCCCATCGGCGACGGCCC CGTGCTGCTGCCCGACAACCACTACCTGAGCACCCAGTCCGCCCTGAGCAA AGACCCCAACGAGAAGCGCGATCACATGGTCCTGCTGGAGTTCGTGACCGC CGCCGGGATCTAA
lacI_GGA_safe	ATGAAACCAGTAACGTTATACGATGTCGCAGAGTATGCCGGTGTCTCTTATC AGACCGTTTCCCGCGTGGTGAACCAGGCCAGCCACGTTTCTGCGAAAACGC GGGAAAAAGTGGAAGCGGCGATGGCGGAGCTGAATTACATTCCCAACCGCG TGGCACAACAACTGGCGGGCAAACAGTCGTTGCTGATTGGCGTTGCCACCT CCAGTCTGGCCCTGCACGCGCCGTCGCAAATTGTCGCGGCGATTAAATCTCG

	CGCCGATCAACTGGGTGCCAGCGTGGTGGTGTCGATGGTAGAACGAAGCGG CGTCGAAGCCTGTAAAGCGGCGGTGCACAATCTTCTCGCGCAACGCGTCAG TGGGCTGATCATTAACTATCCGCTGGATGACCAGGATGCCATTGCTGTGGAA GCTGCCTGCACTAATGTTCCGGCGTTATTTCTTGATGTCTCTGACCAGACAC CCATCAACAGTATTATTTTCTCCCATGAGGACGGTACGCGACTGGGCGTGGA GCATCTGGTCGCATTGGGTCACCAGCAAATCGCGCTGTTAGCGGGCCCATTA AGTTCTGTCTCGGCGCGTCTGCGTCTGGCTGGCTGGCATAAATATCTCACTC GCAATCAAATTCAGCCGATAGCGGAACGGGAAGGCGACTGGAGTGCCATGT CCGGTTTTCAACAAACCATGCAAATGCTGAATGAGGGCATCGTTCCCACTGC GATGCTGGTTGCCAACGATCAGATGGCGCTGGGCGCAATGCGCGCCATTAC CGAGTCCGGGCTGCGCGTTGGTGCGGATATCTCGGTAGTGGGATACGACGA TACCGAGGACAGCTCATGTTATATCCCGCCGTTAACCACCATCAAACAGGAT TTTCGCCTGCTGGGGCAAACCAGCGTGGACCGCTTGCTGCAACTCTCTCAGG GCCAGGCGGTGAAGGGCAATCAGCTGTTGCCCGTCTCACTGGTGAAAAGAA AAACCACCCTGGCGCCCAATACGCAAACCGCCTCTCCCCGCGCGTTGGCCG ATTCATTAATGCAGCTGGCACGACAGGTTTCCCGACTGGAAAGCGGGCAGT GA
tetR	ATGTCTAGATTAGATAAAAGTAAAGTGATTAACAGCGCATTAGAGCTGCTT AATGAGGTCGGAATCGAAGGTTTAACAACCCGTAAACTCGCCCAGAAGCTA GGTGTAGAGCAGCCTACATTGTATTGGCATGTAAAAAATAAGCGGGCTTTG CTCGACGCCTTAGCCATTGAGATGTTAGATAGGCACCATACTCACTTTTGCC CTTTAGAAGGGGAAAGCTGGCAAGATTTTTTACGTAATAACGCTAAAAGTTT TAGATGTGCTTTACTAAGTCATCGCGATGGAGCAAAAGTACATTTAGGTACA CGGCCTACAGAAAAACAGTATGAAACTCTCGAAAATCAATTAGCCTTTTTAT GCCAACAAGGTTTTTCACTAGAGAATGCATTATATGCACTCAGCGCTGTGGG GCATTTTACTTTAGGTTGCGTATTGGAAGATCAAGAGCATCAAGTCGCTAAA GAAGAAAGGGAAACACCTACTACTGATAGTATGCCGCCATTATTACGACAA GCTATCGAATTATTTGATCACCAAGGTGCAGAGCCAGCCTTCTTATTCGGCC TTGAATTGATCATATGCGGATTAGAAAAACAACTTAAATGTGAAAGTGGGT CTTAA
linker sequence for tetR-deGFP fusion	GGTGAAAACCTGTACTTCCAGTCTGGTGGTGCT

Primers to make linear sequences and other plasmids

CHA-R	TTTTATCTAATCTAGACATGTGGTATATCTC CTTCTTAAAGTTAA	Isothermal assembly piece 1 to make 109, 2 w/ ZS30432f
CHB	TTTAAGAAGGAGATATACCACATGTCTAGA TTAGATAAAAGTAAAGTGAT	Isothermal assembly piece 2 to make 109, 3 w/ CHB-R
CHB-R	ACCAGACTGGAAGTACAGGTTTTCACCAGA CCCACTTTCACATTTAAGT	Isothermal assembly piece 2 to make 109, 3 w/ CHB
CHC	AACCTGTACTTCCAGTCTGGTGGTGCTATGG AGCTTTTCACTGGC	Isothermal assembly piece 3 to make 109, 21 w/ CHC-R
CHC-R	CTTTGAGTGAGCTGATACCGCAGTCATAAG TGCGGCGA	Isothermal assembly piece 3 to make 109, 21 w/ CHC
CHD	CGTCGCCGCACTTATGACTGCGGTATCAGCT CACTCAAAG	Isothermal assembly piece 4 to make 109, 105 w/ ZS30432r
ZS3033f	TGAGCTAACACCGTGCGT	0 bp protection, 21 w/ ZS3033rb
ZS3033rb	ACAGAAAAGCCCGCCTTTCGGCGGGCTTTG CTCGAGTTAGATC	0 bp protection, 21 w/ ZS3033f
ZS3034f	CATGCTGAGCTAACACCG	5 bp protection, 21 w/ ZS3034ra
ZS3034ra	TCGACACAGAAAAGCCCG	5 bp protection, 21 w/ ZS3034f
ZS3035f	GTGTGTGCTGTTCCGCT	25 bp protection, 21 w/ ZS3035r
ZS3035r	AAGGCTCTCAAGGGCATC	25 bp protection, 21 w/ ZS3035f
ZS3036f	AAAACCGAATTTTGCTGG	100 bp protection, 21 w/ ZS3036r
ZS3036r	ATGATAAAGAAGACAGTCATAAGTGCG	100 bp protection, 21 w/ ZS3036f
ZS3037f	TGGCGAATCCTCTGACC	250 bp protection, 21 w/ ZS3037r or 121-133 w/ ZS30610r or 58, 134-137 w/ ZS3037r
ZS3037r	TCTTTCCTGCGTTATCCC	250 bp protection, 21 w/ ZS3037f or 134-137 w/ ZS3037f
ZS3038f	AAAGGGAATAAGGGCGACA	500 bp protection, 21 w/ ZS3038r
ZS3038r	AGCGCCACGCTTCCC	500 bp protection, 21 w/ ZS3038f
ZS30412f	TCCGGTGAGCTAACACC	0 bp protection, 87 w/ ZS303412r
ZS30412r	GTTTTACAGAAAAGCCCGC	0 bp protection, 87 w/ ZS303412f
ZS30413f	AGAAGTGAATGATCTACCGGTC	5 bp protection, 87 w/ ZS303413r
ZS30413r	AAGAGCATCCCGACAGC	5 bp protection, 87 w/ ZS303413f
ZS30414f	ATTACTCGCCCCAGAGGTT	25 bp protection, 87 w/ ZS303414r
ZS30414r	GACAAGGTTTCGCGTTG	25 bp protection, 87 w/ ZS303414r
ZS30415f	GTGGGGAAATCTTCTGCC	100 bp protection, 87 w/ ZS303415r
ZS30415r	CGGCGGGCGATAAAC	100 bp protection, 87 w/ ZS303415f
ZS30416f	GCTACGGCATCATCAGTC	250 bp protection, 87 w/ ZS303416r
ZS30416r	GGTGATGGTGTTGATTTCAC	250 bp protection, 87 w/ ZS303416f
ZS30417f	ACGGTGGCGAAATTCA	500 bp protection, 87 w/ ZS303417r
ZS30417r	GAAGCACAGGCCCACTAC	500 bp protection, 87 w/ ZS303417f
ZS30432f	ATGACTATCGCACCATCAGCTAACGATATC CGCCTGAT	Isothermal assembly piece 1 to make 109, 2 w/ CHA-R
ZS30432r	GCATCAGGCGGATATCGTTAGCTGATGGTG CGATAGTCA	Isothermal assembly piece 4 to make 109, 21 w/ CHD
ZS30433f	ATCTAGGTCTCTAACGATATCCGCCTGAT	GGA piece 1 to make 109, 2 w/ ZS30433r
ZS30433r	GTTATGGTCTCGACATGTGGTATATCTCCTT CTTAAAGTTAA	GGA piece 1 to make 109, 2 w/ ZS30433f
ZS30434f	GATACGGTCTCCATGTCTAGATTAGATAAA AGTAAAGTGAT	GGA piece 2 to make 109, 3 w/ ZS3081r

ZS30435r	GTGCCGGTCTCATACCGCAGTCATAAGTGC GGCGA	GGA piece 3 to make 109, 21 w/ ZS3081f
ZS30436f	GGTTTGGTCTCCGGTATCAGCTCACTCAAAG	GGA piece 4 to make 109, 105 w/ ZS30436r
ZS30436r	ACGTTGGTCTCTCGTTAGCTGATGGTGCGAT AGTC	GGA piece 4 to make 109, 105 w/ ZS30436f
ZS30512f	AACAGGGTCTCACATGGAGCTTTTCACTGG	GGA “C7”, “C8”, 21 w/ ZS30523r or 18 w/ ZS30523r
ZS30513r	GTCCGGGTCTCACGACTCTCAAGGGCATCG GT	GGA “T2”, 21 w/ ZS30524f
ZS30514f	GTCCTGGTCTCTATGCGTGGTTGTCTTCGTA CGTCCGTCACGTTC	GGA “v1-1”, 105 w/ ZS30514r
ZS30514r	ATATAGGTCTCTGTCGGGCATTGTCTTCGCT CCTTCCGGTGG	GGA “v1-1”, 105 w/ ZS30514f
ZS30515f	TAGCGGGTCTCTGTCGTGCCTTGTCTTCGTT ACGTCCGTCACGTTC	GGA “v1-2”, 105 w/ ZS30528r
ZS30521r	CGTAAGGTCTCAGCTTGCTGTGCTCAGTATC TCT	GGA “P4”, 2 w/ ZS3057f
ZS30522f	AGCCAGGTCTCAAAGCAATAATTTTGTTTA ACTT	GGA “U2”, 21 w/ ZS3059r
ZS30523r	TTAGTGGTCTCATTCATTAGATCCCGGCGGC	GGA “C7”, “C8”, 21 w/ ZS30512f or 18 w/ ZS30512f
ZS30524f	GGCTCGGTCTCATGAAGCATCTGGTGAATA ACTCGAG	GGA “T2”, 21 w/ ZS30513r
ZS30528r	AGGTGGGTCTCTATGCTATGTTGTCTTCGCT CCTTCCGGTGG	GGA “v1-2”, 105 w/ ZS30515f
ZS30534r	CGTAAGGTCTCAGCTTGCTGTGCTCAGTATC TTGT	GGA “P3”, 3 w/ ZS3057f
ZS3057f	AGAACGGTCTCAGCATTGCTGTTCCGCTGG	GGA “P3”, “P4”, 3 w/ ZS30534r or 2 w/ ZS30521r
ZS3059r	TCCCCGGTCTCACATGGTATATCTCCTTCTT A	GGA “U2”, 21 w/ ZS30522f
ZS30610r	GAAGATCATCTTATTAATCAGATAAAATAT	250 bp protection, 121-133 w/ ZS3037f
ZS30611f	ACGAGGCCCTTTCGTCT	250 bp protection, 109 w/ ZS30611r
ZS30611r	ACGAGGCCCTTTCGTCT	250 bp protection, 109 w/ ZS30611f
ZS3064f	T*G*AGCTAACACCGTGCGT	0 bp protection, 2 TS, 21 w/ ZS3064r
ZS3064r	A*C*AGAAAAGCCCGCCTTTCGGCGGGCTTT GCTCGAGTTAGATC	0 bp protection, 2 TS, 21 w/ ZS3064f
ZS3065f	T*G*A*G*C*TAACACCGTGCGT	0 bp protection, 5 TS, 21 w/ ZS3065r
ZS3065r	A*C*A*G*A*AAAGCCCGCCTTTCGGCGGGC TTTGCTCGAGTTAGATC	0 bp protection, 5 TS, 21 w/ ZS3065f
ZS3066f	C*A*TGCTGAGCTAACACCG	5 bp protection, 2 TS, 21 w/ ZS3066r
ZS3066r	T*C*GACACAGAAAAGCCCGCCTTTCGGCGG GCTTTGCTCG	5 bp protection, 2 TS, 21 w/ ZS3066f
ZS3067f	C*A*T*G*C*TGAGCTAACACCG	5 bp protection, 5 TS, 21 w/ ZS3067r
ZS3067r	T*C*G*A*C*ACAGAAAAGCCCGCCTTTCGG CGGGCTTTGCTCG	5 bp protection, 5 TS, 21 w/ ZS3067f
ZS3068f	T*G*GCGAATCCTCTGACC	250 bp protection, 2 TS, 21 w/ ZS3068r
ZS3068r	T*C*TTTCCTGCGTTATCCC	250 bp protection, 2 TS, 21 w/ ZS3068f
ZS3069f	T*G*G*C*G*AATCCTCTGACC	250 bp protection, 5 TS, 21 w/ ZS3069r

ZS3069r	T*C*T*T*T*CCTGCGTTATCCC	250 bp protection, 5 TS, 21 w/ ZS3069f
ZS3071f	/5Alex594N/TGGCGAATCCTCTGACC	250 bp protection, 5' AF594, 21 w/ ZS3071r
ZS3071r	/5Alex594N/TCTTTCCTGCGTTATCCC	250 bp protection, 5' AF594, 21 w/ ZS3071f
ZS30810f	CAACCACGCATTGCTGTT	Overlap primers on "v1-1", 134-135 w/ ZS30810r
ZS30810r	CAATGCCCGACTCTCAAG	Overlap primers on "v1-1", 134-135 w/ ZS30810f
ZS30811f	CAAGGCACGACTCTCAAG	Overlap primers on "v1-2", 136-137 w/ ZS30811f
ZS30811r	ACAACATAGCATTGCTGTTC	Overlap primers on "v1-2", 136-137 w/ ZS30811r
ZS3081f	TCCTTGGTCTCGCTTCCAGTCTGGTGGTGCTATGGAGCTTTTCACTGGC	GGA piece 3 to make 109, 21 w/ ZS30435r
ZS3081r	TAACCGGTCTCAGAAGTACAGGTTTTCACCAGACCCACTTTCACATTTAAGT	GGA piece 2 to make 109, 3 w/ ZS30434f

Supplemental S3.

Inducible promoters Pl-tetO1 and Pl-lacO1 in linear and plasmid DNA were fit to a standard Hill function to approximate Michaelis-Menten dynamics using Prism 6.0 software (GraphPad Software, Inc.), which assumes a hill slope of 1.0:

$$[\boldsymbol{deGFP}] = \frac{\boldsymbol{V_{max}}[\boldsymbol{inducer}]}{\boldsymbol{K_m} + [\boldsymbol{inducer}]}$$

Table S1. Comparing absorbance and fluorometric quantifications of linear and plasmid DNA. (numerical). Data from Figure S1 in numerical form, with percent error from expected value included.

Linear	**Nanodrop**		**BR linear standard**		**HS linear standard**	
Expected (ng/μL)	Actual (ng/μL)	% Error	Actual (ng/μL)	% Error	Actual (ng/μL)	% Error
500	490.8 +/ 4.2	1.84%	471.7 +/- 41.3	5.67%		
250	251.3 +/- 2.1	0.53%	229.7 +/- 2.5	8.13%		
125	126.7 +/- 3.6	1.36%	114.7 +/- 1.2	8.27%	55	56.00%
62.5	63.80 +/- 3.10	2.08%	53.63 +/-2.24	10.99%	55.33 +/- 1.15	11.47%
31.25	32.87 +/- 2.61	5.17%	27.73 +/- 2.00	11.25%	28.07 +/- 2.38	10.19%
15.625	17.33 +/- 1.99	10.93%	13.97 +/- 1.40	10.61%	13.77 +/- 1.76	11.89%
7.8125	9.60 +/- 1.84	22.88%	6.97 +/- 0.92	10.74%	7.02 +/- 1.09	10.14%
3.90625	5.67 +/- 1.50	45.07%	3.51 +/- 0.82	10.06%	3.44 +/- 0.69	12.02%
1.953125	3.70 +/- 0.82	89.44%	1.77 +/- 0.54	9.38%	1.78 +/- 0.32	8.86%
0.976563	2.50 +/- 1.13	156.00%	1.17 +/- 0.05	19.30%	0.91 +/- 0.15	6.65%

Plasmid	**Nanodrop**		**BR linear standard**		**HS linear standard**		**BR plasmid standard**		**HS plasmid standard**	
Expected (ng/μL)	Actual (ng/μL)	% Error	Actual (ng/μL)	% Error	Actual (ng/μL)	% Error	Actual (ng/μL)	% Error	Actual (ng/μL)	% Error
500	494.2 +/- 7.1	1.15%	516.0 +/- 24.3	3.20%			556.7 +/- 47.3	11.33%		
250	255.7 +/- 4.6	2.28%	244.7 +/- 6.4	2.13%			260.7 +/- 18.0	4.27%		
125	128.9 +/- 5.3	3.15%	122.0 +/- 7.5	2.40%			124.0 +/- 3.5	0.80%		
62.5	64.87 +/- 4.02	3.79%	59.90 +/- 4.16	4.16%	46.43 +/- 6.93	25.71%	61.10 +/- 3.47	2.29%		
31.25	32.83 +/- 3.32	5.07%	29.43 +/- 3.40	5.81%	19.10 +/- 0.72	38.88%	29.37 +/- 1.01	6.03%	27.13 +/- 1.93	13.17%
15.625	16.83 +/- 2.50	7.73%	14.83 +/- 2.11	5.07%	8.57 +/- 0.85	45.13%	14.53 +/- 0.74	6.99%	12.77 +/- 1.50	18.29%
7.8125	8.67 +/- 2.23	10.93%	7.54 +/- 1.19	3.49%	4.02 +/- 0.28	48.50%	7.32 +/- 0.31	6.26%	5.70 +/- 0.75	27.04%
3.90625	4.57 +/- 1.70	16.91%	3.75 +/- 0.87	4.00%	1.99 +/- 0.20	49.14%	3.52 +/- 0.26	9.97%	2.90 +/- 0.22	25.76%
1.953125	2.80 +/- 1.73	43.36%	1.88 +/- 0.57	3.57%	0.99 +/- 0.06	49.33%	1.84 +/- 0.17	5.96%	1.44 +/- 0.07	26.27%
0.976563	1.60 +/- 1.40	63.84%	1.17 +/- 0.11	19.81%	0.50 +/- 0.04	48.77%	1.12	14.69%	0.72 +/- 0.08	26.48%

Table S2. Time Estimates of a Test Cycle in TX-TL. Time needed for rapid assembly in vitro versus traditional cloning, corresponding to Figure 6, is presented.

	Rapid Assembly[1]	Conventional Techniques (plasmid generation)
PCR of segments	na	1 h 15 min
DpnI digest[2, 3]	na	5 min
Assembly reaction[4]	1 h	1 h
Transformation and Recovery	na	1 h 30 min
Overnight growth on plates	na	16 h
Colony isolation and liquid media growth	na	8 h
Miniprep	na	30 min
PCR of rapid assembly product	1 h 15 min	
PCR Cleanup[3]	15 min	15 min
Setup TX-TL	15 min	15 min
TOTAL pre-TX-TL	2 h 45 min	1 d +
TOTAL post-TX-TL	4 h – 8 h	1 d +

[1] Rapid Assembly assumes the use of premade, re-usable modular parts – if these are not available, add 1 h 20 min to predicted time and follow beginning of "Conventional Techniques" protocol.

[2] Assumes the use of a fast-digest enzyme.

[3] During digest, run the previous reaction on an agarose gel to determine purity and reaction completion.

[4] Golden Gate Assembly has multiple protocols, from 1h to 3h20min in length. Protocol listed here assumes 10 cycles of 2min/37°C, 3min/20°C, 1 cycle 5min/50°C, 5min/80°C. Difficult assemblies can be accomplished by increasing cycling steps or by doing a constant at 37°C. Isothermal assembly can also be used in lieu.

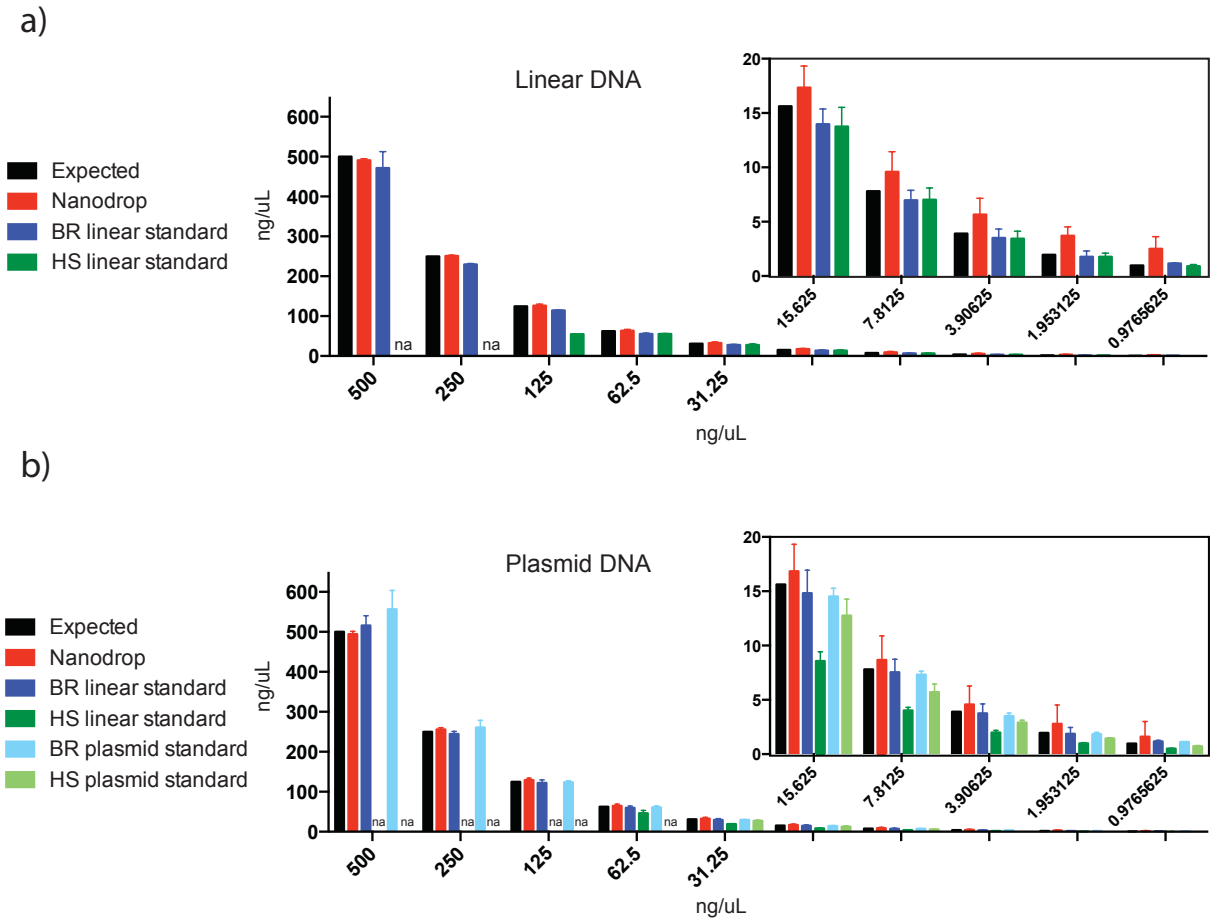

Figure S1. Comparing spectrophotomeric and fluorometric quantifications of linear and plasmid DNA. (graphic). a) 2 μL of 1kb linear ladder DNA at the expected ng/μL was either measured in the Nanodrop or the Qubit fluorometer using the dsDNA BR assay or dsDNA HS assay. Error bars represent a standard deviation from three independent samples, and "na" indicates out of range of the machine. b) Same process as a), but with supercoiled plasmid ladder DNA. BR linear standard: supplied with Qubit dsDNA BR Assay kit; HS linear standard: supplied with Qubit dsDNA HS Assay kit; BR plasmid standard: pUC19 plasmid DNA of known concentration at 0 ng/μL and 100 ng/μL in TE buffer; HS plasmid standard: pUC19 at 0 ng/μL and 10 ng/μL in TE buffer.

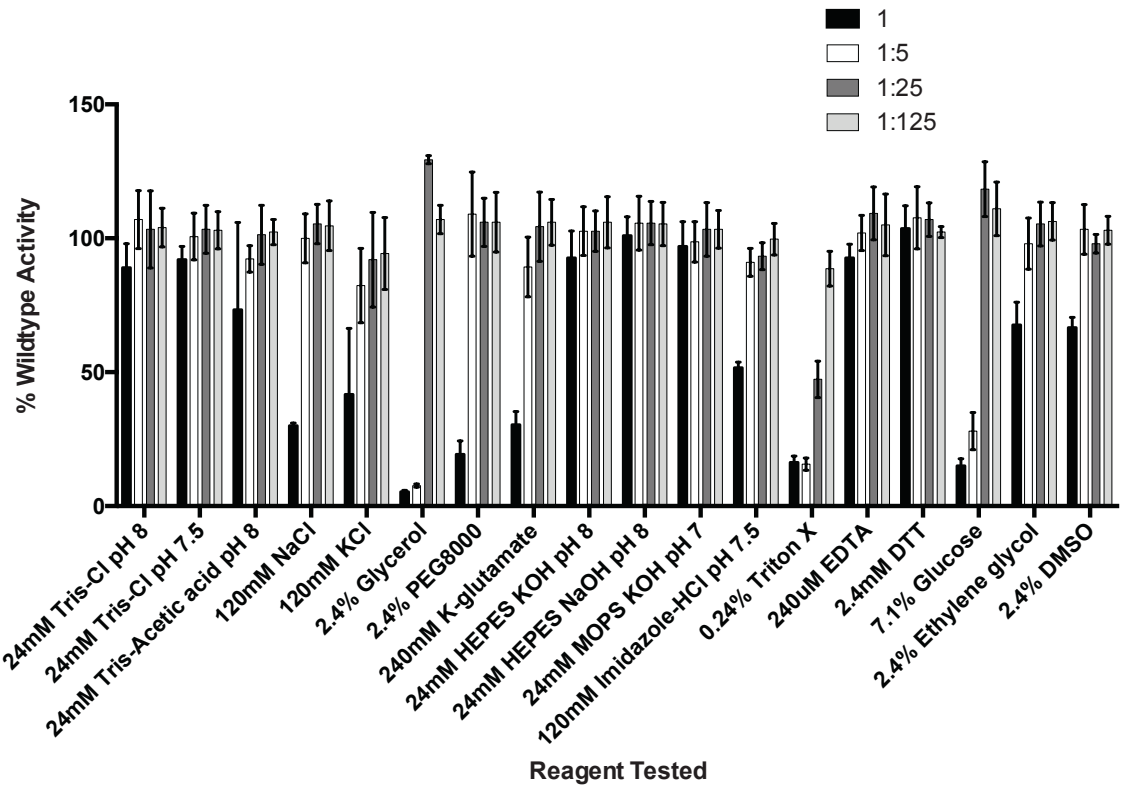

Figure S2. Effects of different additives on TX-TL efficiency. A variety of different additives commonly used in protein buffers was tested for toxicity. Endpoint fluorescence after 8 hours was determined for 1nM of pBEST-OR2-OR1-Pr-UTR1-deGFP-T500 at the final working concentrations listed in TX-TL or at 1:5 dilutions. Percent wildtype activity is against a control with no additive. Error bars represent one standard deviation from three independent experiments. Experiment is done in extract "e10."

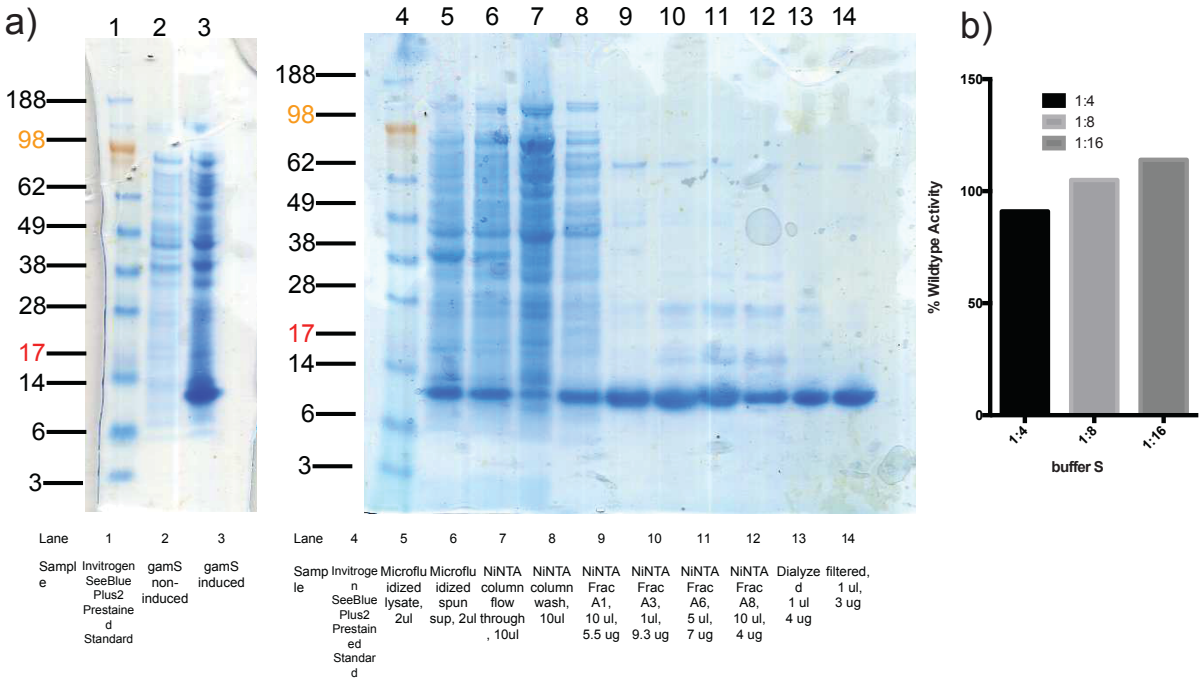

Figure S3. Purification of lambda gam protein into lambda gam storage buffer S. a) Lambda gam protein was purified, expressed, and concentrated into 3 mg/ml as described in "Materials and Methods." Shown is the Coomassie Brilliant Blue stain of the purification procedure. b) Buffer toxicity of lambda gam storage buffer in TX-TL at different dilutions. Storage buffer composition ("buffer S") is 50 mM Tris-Cl pH 7.5, 100 mM NaCl, 1 mM DTT, 1 mM EDTA, 2% DMSO. Experiment is done in extract "e10."

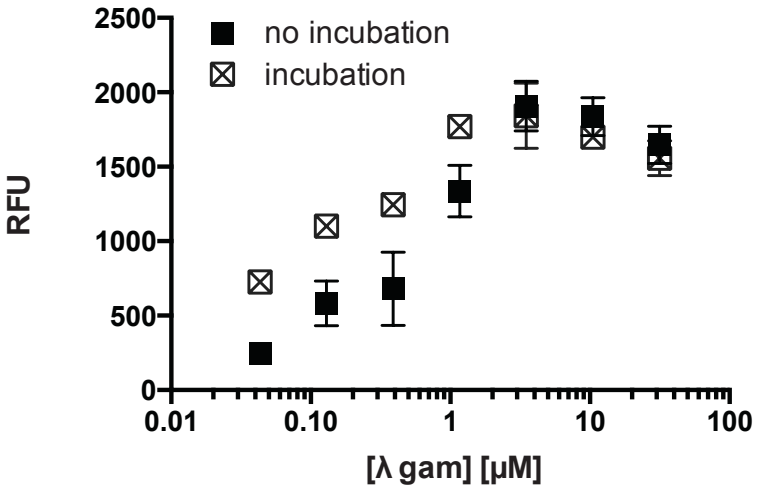

Figure S4. Effect of incubation time of lambda gam protein on linear protection. Lambda gam protein to the listed concentration was added either directly to the crude cell extract for 30 minutes at room temperature ("incubation," square-x) or directly to the DNA ("no incubation," black-x). In the "incubation" case, crude cell extract incubated with lambda gam protein was then moved to 4°C and added to DNA. In the "no incubation" case, crude cell extract at 4°C was added directly to a mix of DNA and lambda gam protein. Reaction was run with 2 nM of linear DNA with no protection, and deGFP endpoint signal was measured. Error bars represent one standard deviation from three independent experiments.

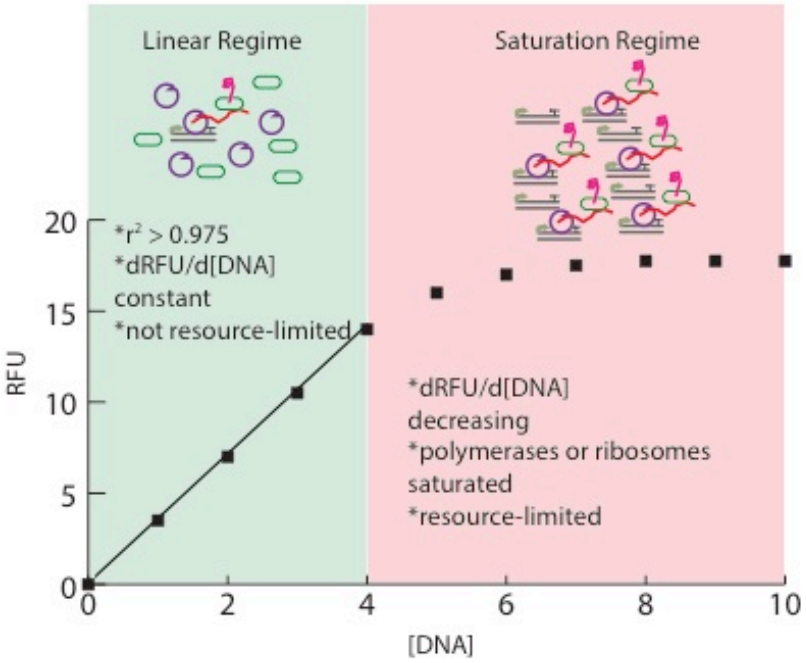

Figure S5. Definition of linear regime and saturation regime in TX-TL. Cartoon diagram shows hypothetical reaction with reporter protein, where rate of signal increase with DNA is constant up to 4 nM ("linear regime", green), begins to slow from 4 nM to 7 nM before becoming 0 above 7 nM ("saturation regime," red). The linear regime is not resource-limited, while the saturation regime is resource limited. Purple semicircle: RNA polymerase; green oval: ribosome; grey lines: DNA; red line: mRNA; pink squiggly: protein.

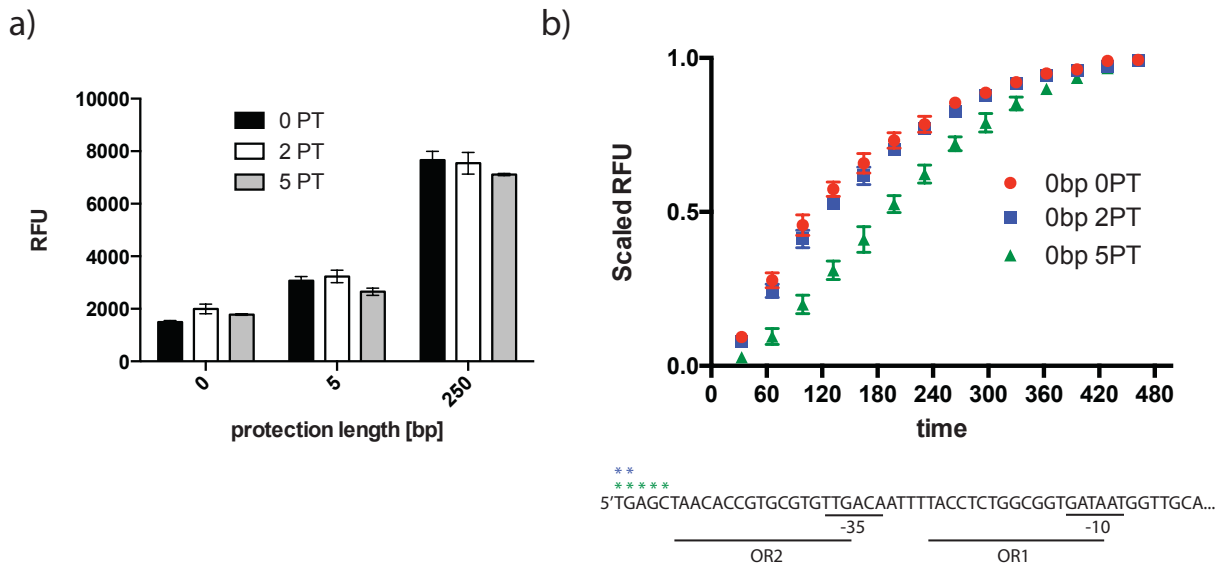

Figure S6. Protection of linear constructs with varying amounts of phosphorothioates. a) Endpoint expression of 2 nM linear DNA with 0, 2, or 5 phosphorothioates ("PT") on the 5" end on constructs with 0 bp, 5 bp, or 250 bp of non-coding DNA protection. b) Top, time-series data of expression from 2nM of a linear DNA construct with no non-coding sequence protection on either side of promoter OR2-OR-Pr and of terminator. All data series are scaled to an endpoint expression of 1.0 after 8 hours. Below, nucleotide sequence of the left side of the construct, with operator, promoter -35 and -10, and phosphorothioate sites notated [2]. Error bars represent one standard deviation from three independent experiments.

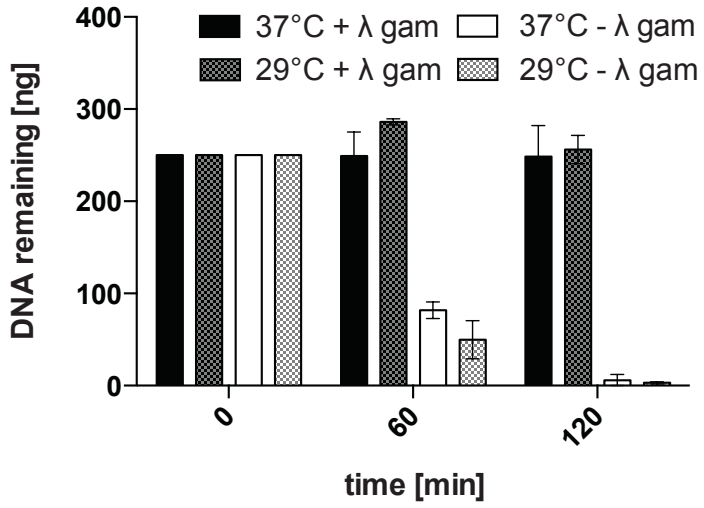

Figure S7. Degradation of saturating amounts of DNA in extracts prepared at different temperatures with and without lambda gam protein. Degradation rates of 250 ng (20 nM) of linear DNA with AlexaFluor-584 labeled dUTPs over time in extract produced at 37°C (extract "eZS1") or 29°C (extract "e13"). Signal is scaled to maximum DNA levels at time t=0. Error bars represent one standard deviation from three independent experiments.

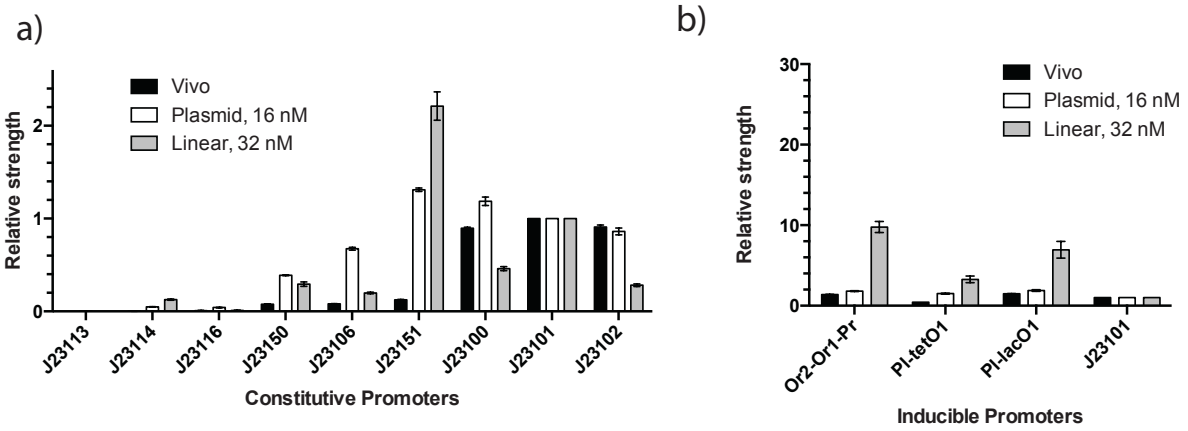

Figure S8: Comparison of strengths of different promoters in a TX-TL saturation regime. a) Figure 4a was repeated for constitutive promoters but using saturating amounts of plasmid and linear DNA. b) Figure 4b was repeated for inducible promoters expressed constitutively.

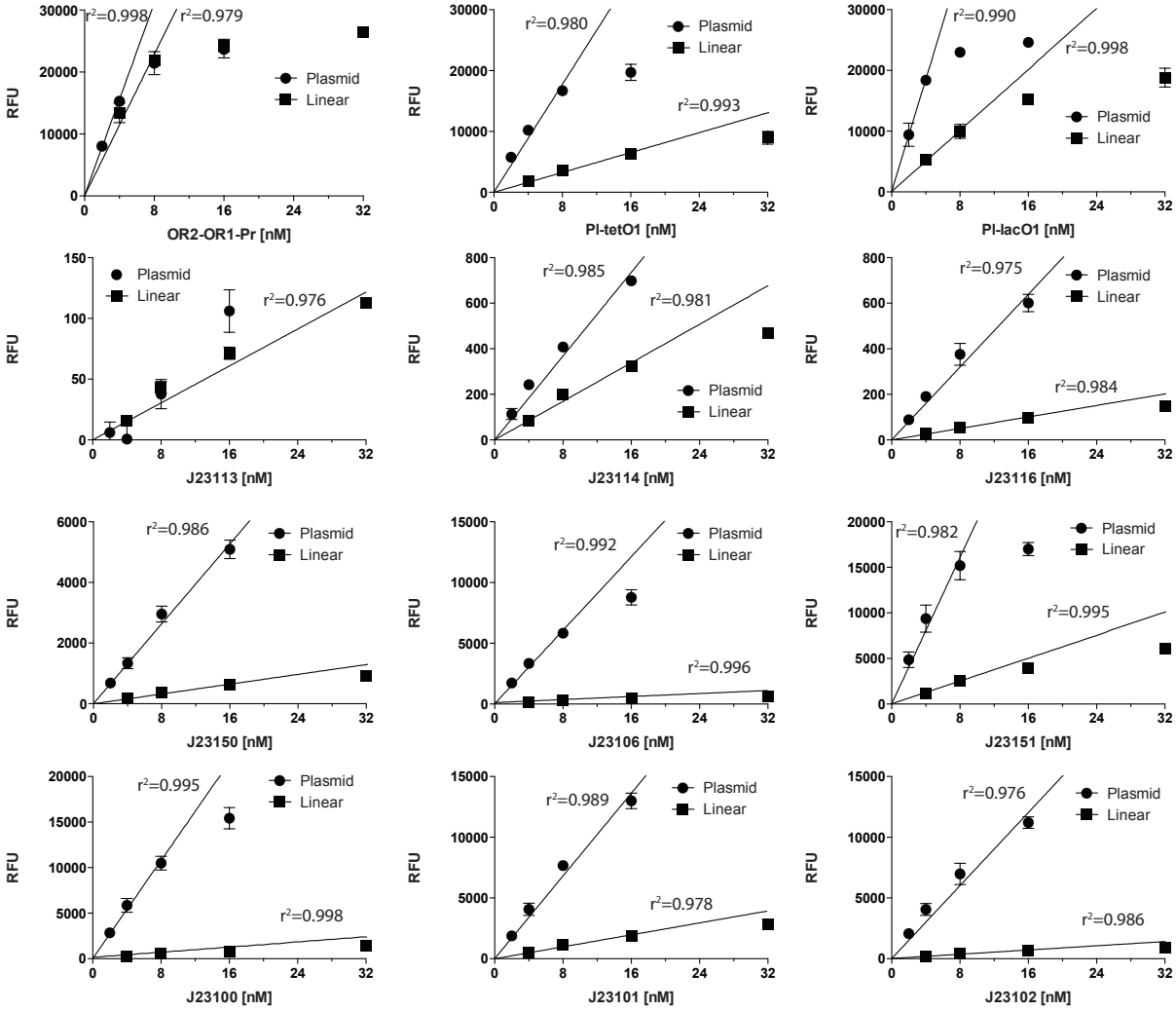

Figure S9. Individual traces of saturation curves. Saturation curves similar to Figure 4d, plotted for all promoters. r^2 and linear regression line are based on a cutoff of 0.975 and correspond to data from Table 1. Linear DNA was protected with 250bp of steric protection and with lambda gam. Error bars represent one standard deviation from three independent experiments.

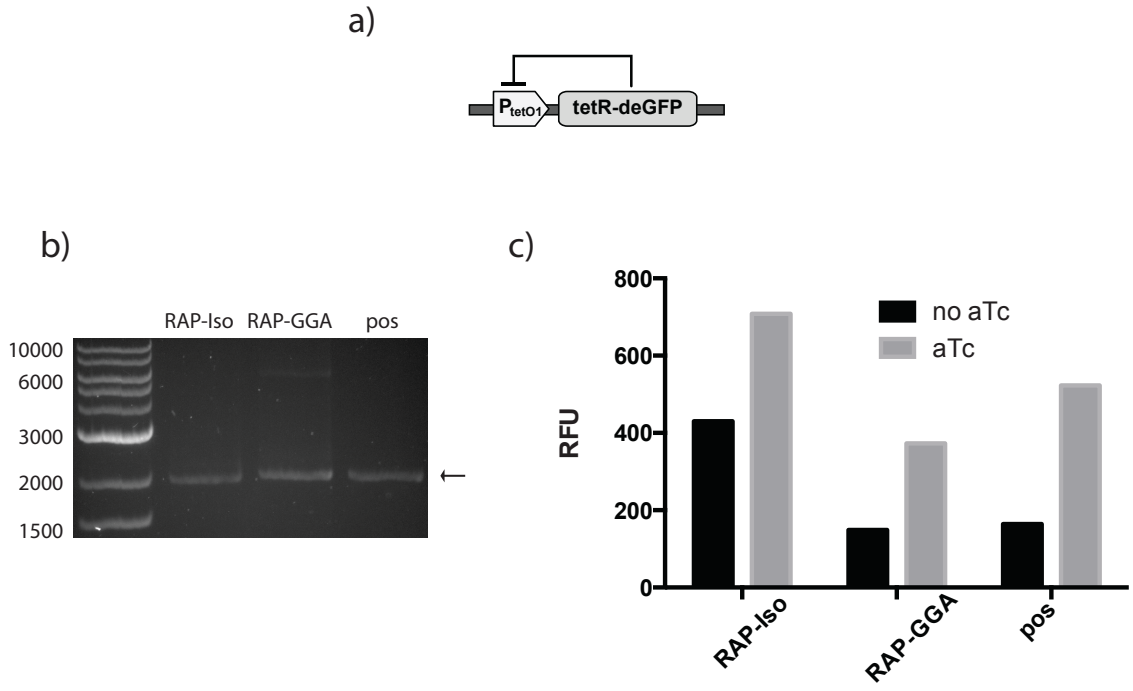

Figure S10. Rapid assembly and testing of a negative feedback gene. a) A four-piece negative feedback gene was assembled from standard pieces. b) Comparison by agarose gel electrophoresis of rapid assembly product made by Isothermal assembly ("RAP-iso"), rapid assembly product made by Golden Gate assembly ("RAP-GGA"), and post-cloned PCR product ("pos"). Arrow indicates expected band. Constructs have 250bp of protection. c) Functional testing of 6 nM of rapid assembly products compared to post-cloned PCR product with or without 10 μM aTc.

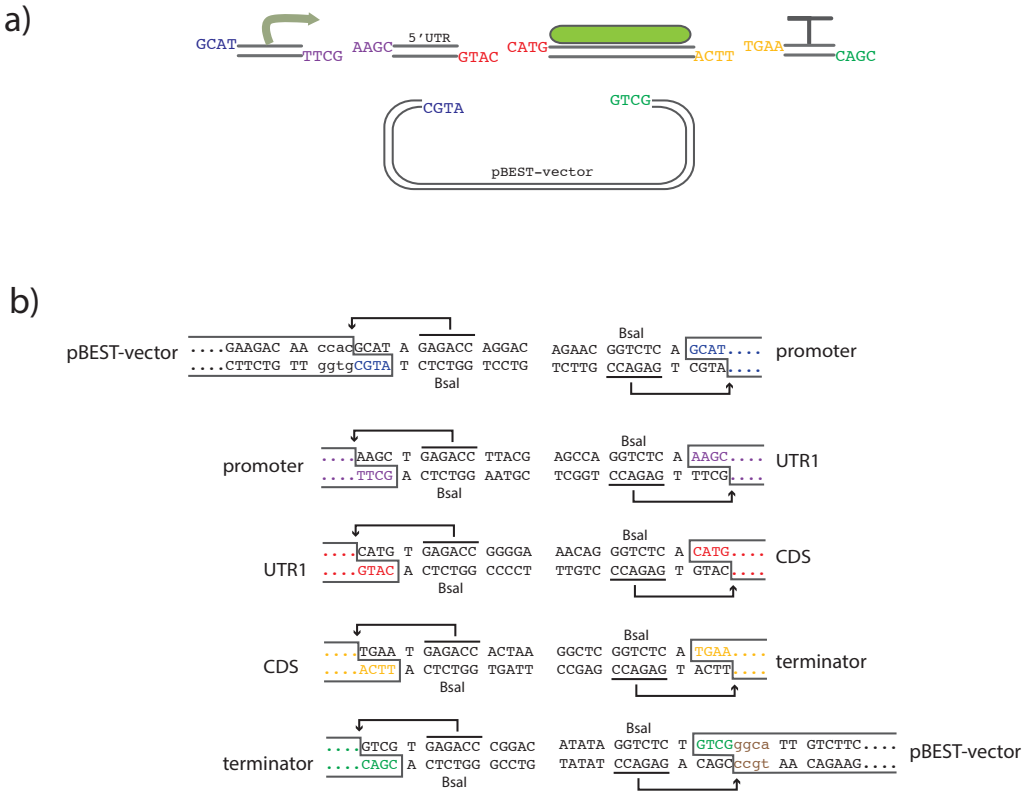

Figure S11. Overview of standard cloning procedure. a) A five piece standard adopted with specific ligation ends for a promoter, 5' UTR, coding sequence, terminator, and vector based on the previously used pBEST backbone. b) Diagram of sequences for ligation at each site.

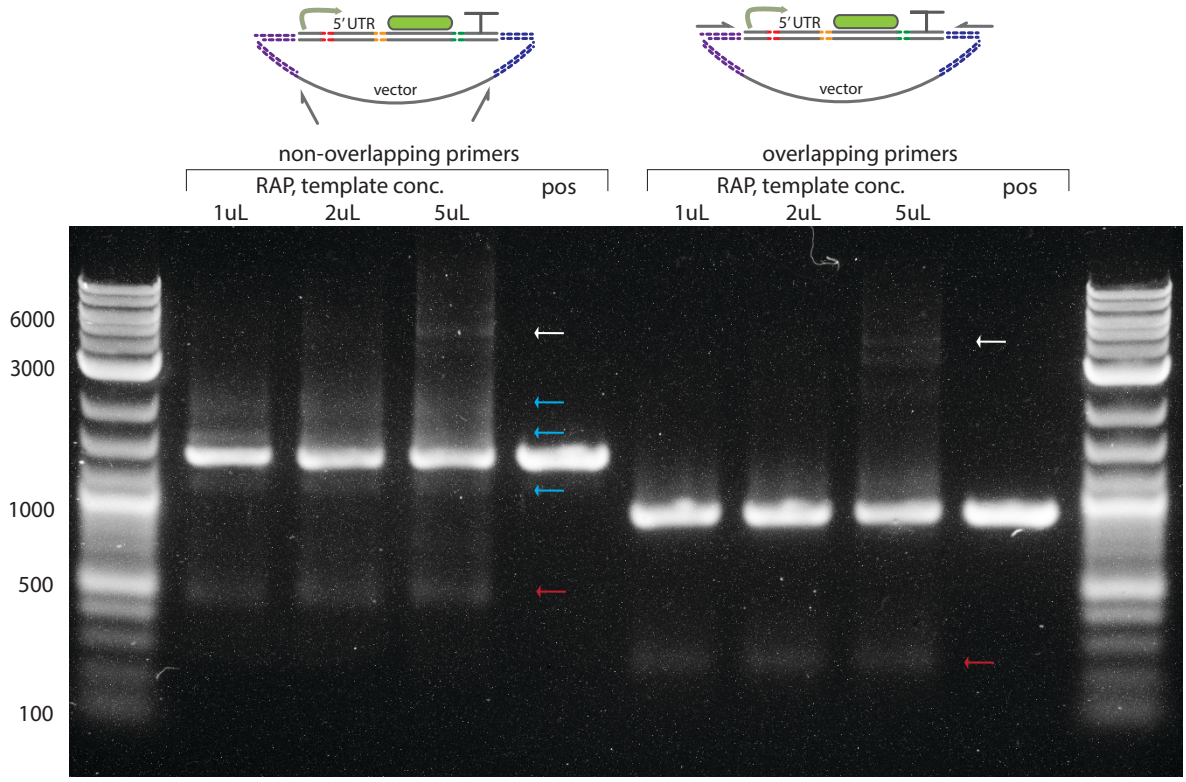

Figure S12. Purity of rapid assembly product as a function of template concentration and of overlapping primers. For a standard 5-piece assembly, the rapid assembly product ("RAP") is amplified off either 1 μL, 2 μL, or 5 μL of template in a 50 μL PCR reaction. A post-cloned PCR product ("pos") is also produced. Non-overlapping primers refer to binding sites which do not cross the assembly junction between the vector and promoter and the vector and terminator; overlapping primers cross this junction. White arrow: template DNA; Blue arrows: Non-specific products removed by overlapping primers; Red arrow: non-specific products retained by overlapping primers. Red arrow is presumed to be self-ligated vector based on size.

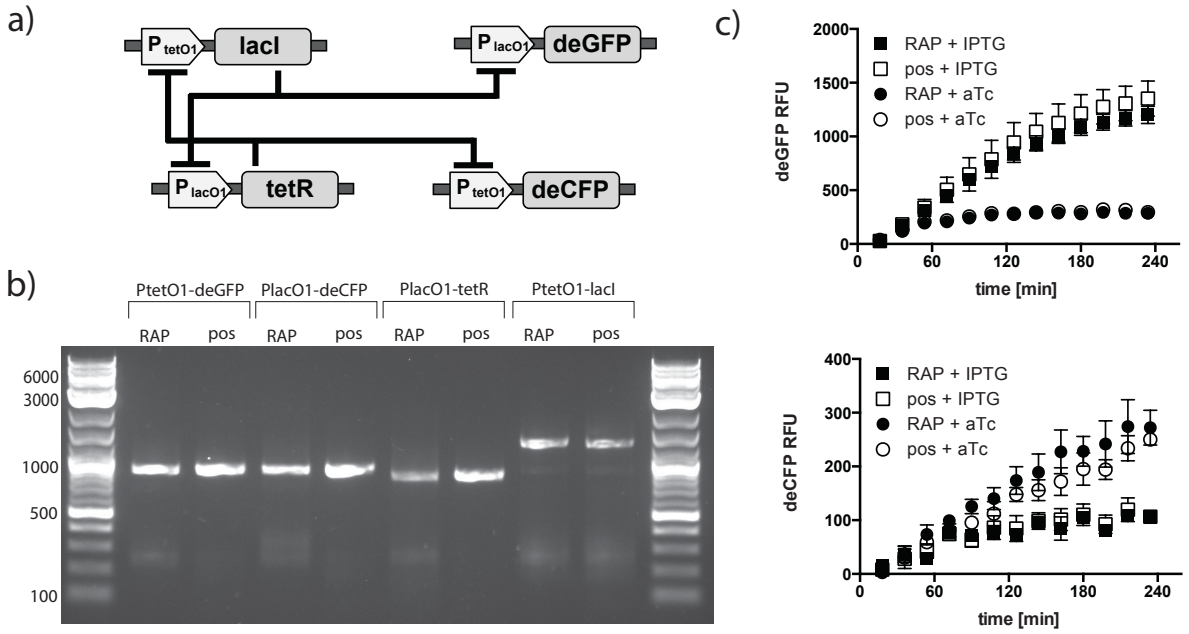

Figure S13: Rapid assembly of genetic switch. a) A four-piece genetic switch, identical to that in Figure 5a. b) Comparison of rapid assembly product ("RAP") to post-cloned PCR product ("pos") for four linear pieces formed, using overlap primers. Constructs have 31 bp of steric protection on each side. c) Functional assay of RAP products versus post-cloned PCR products for "on" or "off" states of genetic switch. 2 nM of reporter and 1 nM of repressor is tested, and "+ IPTG" indicates the 0.5 mM IPTG, 0 μM aTc state while "- IPTG" indicates the 0 mM IPTG, 10 μM aTc state. Error bars represent one standard deviation from three independent experiments.

Supplementary Information References:

1. Labarca, C. and K. Paigen, *A simple, rapid, and sensitive DNA assay procedure.* Anal Biochem, 1980. **102**(2): p. 344-52.
2. Meyer, B.J., R. Maurer, and M. Ptashne, *Gene regulation at the right operator (OR) of bacteriophage lambda. II. OR1, OR2, and OR3: their roles in mediating the effects of repressor and cro.* J Mol Biol, 1980. **139**(2): p. 163-94.